



Acidic pH and divalent cation sensing by PhoQ are dispensable for systemic salmonellae virulence

Kevin G Hicks¹, Scott P Delbecq², Enea Sancho-Vaello³, Marie-Pierre Blanc¹, Katja K Dove², Lynne R Prost⁴, Margaret E Daley⁵, Kornelius Zeth^{6,7}, Rachel E Klevit², Samuel I Miller^{1,8,9*}

¹Department of Microbiology, University of Washington Medical School, Seattle, United States; ²Department of Biochemistry, University of Washington Medical School, Seattle, United States; ³Unidad de Biofísica, Centro Mixto Consejo Superior de Investigaciones Científicas-Universidad del País Vasco/Euskal Herriko Unibertsitatea (CSIC,UPV/EHU), Leioa, Bizkaia, Spain; ⁴Department of Biochemistry, University of Wisconsin–Madison, Madison, United States; ⁵Department of Chemistry and Biochemistry, University of San Diego, San Diego, United States; ⁶Department of Biochemistry and Molecular Biology, University of Basque Country, Leioa, Spain; ⁷IKERBASQUE, Basque Research Organisation for Science, Bilbao, Spain; ⁸Department of Genome Sciences, University of Washington Medical School, Seattle, United States; ⁹Department of Medicine, University of Washington Medical School, Seattle, United States

Abstract *Salmonella* PhoQ is a histidine kinase with a periplasmic sensor domain (PD) that promotes virulence by detecting the macrophage phagosome. PhoQ activity is repressed by divalent cations and induced in environments of acidic pH, limited divalent cations, and cationic antimicrobial peptides (CAMP). Previously, it was unclear which signals are sensed by salmonellae to promote PhoQ-mediated virulence. We defined conformational changes produced in the PhoQ PD on exposure to acidic pH that indicate structural flexibility is induced in α -helices 4 and 5, suggesting this region contributes to pH sensing. Therefore, we engineered a disulfide bond between W104C and A128C in the PhoQ PD that restrains conformational flexibility in α -helices 4 and 5. PhoQ^{W104C-A128C} is responsive to CAMP, but is inhibited for activation by acidic pH and divalent cation limitation. *phoQ*^{W104C-A128C} *Salmonella enterica* Typhimurium is virulent in mice, indicating that acidic pH and divalent cation sensing by PhoQ are dispensable for virulence.

DOI: 10.7554/eLife.06792.001

*For correspondence: millersi@uw.edu

Competing interests: The authors declare that no competing interests exist.


Funding: See page 19

Received: 01 February 2015

Accepted: 22 May 2015

Published: 23 May 2015

Reviewing editor: Feng Shao, National Institute of Biological Sciences, China

 Copyright Hicks et al. This article is distributed under the terms of the [Creative Commons Attribution License](https://creativecommons.org/licenses/by/4.0/), which permits unrestricted use and redistribution provided that the original author and source are credited.

Introduction

Salmonellae are Gram-negative bacterial pathogens that cause severe gastroenteritis and systemic disease in animals and humans. Critical for salmonellae virulence is their ability to survive and replicate within host cells (*Fields et al., 1986*). Following phagocytosis by macrophages, salmonellae are contained within a phagosomal environment containing a diversity of antimicrobial factors including proteases, reactive oxygen and nitrogen species, acidic pH and cationic antimicrobial peptides (CAMP) (*Flannagan et al., 2009*). Salmonellae have multiple mechanisms, including the PhoQ sensor, to sense the phagosomal milieu and respond by increasing their resistance to host antimicrobial factors (*Haraga et al., 2008; Chen and Groisman, 2013; Dalebroux and Miller, 2014*). PhoQ is the sensor kinase component of the PhoPQ two-component regulatory system that governs the

eLife digest *Salmonella* bacteria cause illnesses in humans, such as food poisoning and typhoid fever. In response to a *Salmonella* infection, immune cells known as macrophages detect and engulf the bacteria. The conditions inside the macrophage (which include an acidic pH and high levels of antimicrobial molecules) can destroy some bacteria. However, *Salmonella* bacteria (which are also called salmonellae) can sense and counteract these hostile conditions; this allows them to remodel their surface to survive and reproduce inside macrophages and continue to cause disease.

A protein known as PhoQ, which is found on the surface of *Salmonella* bacteria, is a sensor that detects when the bacterium is inside a macrophage and so needs to boost its defenses. The PhoQ sensor is able to respond to acidity, the absence of divalent cations—such as magnesium and calcium ions—and certain antimicrobial peptide molecules. These conditions and components are used inside macrophages to try and kill the bacteria, but it was not known which of these signals PhoQ actually senses during an infection.

Hicks et al. established how the sensor region of PhoQ changes when it is exposed to acid. This knowledge enabled variants of this protein to be constructed that do not respond when exposed to acidic conditions or low levels of divalent cations. Salmonellae that have these modified PhoQ sensors were still able to infect macrophages and cause disease in mice. These findings suggest that antimicrobial peptide sensing alone is sufficient to trigger the bacteria's defenses inside host organisms.

Understanding how salmonellae detect antimicrobial factors could help with the development of new treatments for the diseases caused by these bacteria. Furthermore, the new tools developed by Hicks et al. could be applied to other systems to characterize how bacteria interact with their host environment during infection.

DOI: [10.7554/eLife.06792.002](https://doi.org/10.7554/eLife.06792.002)

phosphorylated state of the response regulator PhoP (**Groisman et al., 1989; Miller et al., 1989**). PhoQ exists as a dimer within the inner membrane and has a periplasmic sensor domain (PD) that transduces signals across the inner membrane to the cytoplasmic histidine kinase domain. Following activation of PhoQ by the phagosomal environment, PhoP is phosphorylated and transcriptionally controls a large network of genes (>300), many of which are involved in virulence (**Fields et al., 1989; Behlau and Miller, 1993; Belden and Miller, 1994; Gunn and Miller, 1996; Guo et al., 1997; Bearson et al., 1998; Guo et al., 1998; Adams et al., 2001; Bader et al., 2003; Dalebroux et al., 2014**). Precise PhoPQ-mediated gene regulation is essential for salmonellae infection as strains with null or constitutively active mutations in PhoPQ are highly attenuated for virulence in animals and humans (**Fields et al., 1989; Galán and Curtiss, 1989; Miller et al., 1989; Miller and Mekalanos, 1990**).

The PhoQ PD is a member of the PAS-fold and PDC-fold domain families (**Cho et al., 2006; Cheung et al., 2008; Cheung and Hendrickson, 2010**). Unlike other PDC-sensors, which bind small ligands in a defined binding pocket or PhoQ PD homologs found in environmental bacteria, the PhoQ PD from bacteria that primarily interact with animals has no apparent binding pocket due to an occluding structural element: α -helices 4 and 5 (**Cho et al., 2006; Prost et al., 2007; Cheung et al., 2008; Prost et al., 2008**). Acidic residues on α 4 and α 5 and β -strands 5 and 6 in the PhoQ PD form a structural scaffold for binding antimicrobial peptides, as well as the divalent cations Mg^{2+} , Mn^{2+} , and Ca^{2+} (**Waldburger and Sauer, 1996; Bader et al., 2005; Cho et al., 2006; Prost et al., 2008**). PhoQ kinase activity is repressed and phosphatase activity is dominant at millimolar or greater concentrations of divalent cations (**García Vescovi et al., 1996; Castelli et al., 2000; Montagne et al., 2001**), presumably due to divalent cation salt-bridges formed between the PD acidic patch and inner membrane phospholipids (**Cho et al., 2006**). Additionally, PhoQ activity is repressed by feedback inhibition involving the small inner membrane protein, MgrB (**Lippa and Goulian, 2009**). Conversely, bacterial growth in sub-millimolar divalent cation conditions results in PhoQ activation and increased kinase activity (**García Vescovi et al., 1996**), presumably due to disruption of salt-bridges between the PhoQ PD and inner membrane. However, the macrophage phagosome has a magnesium concentration of approximately one millimolar and a calcium concentration of approximately 500 micromolar, suggesting PhoQ is not activated by divalent cation limitation during

intracellular infection (*Christensen et al., 2002; Martin-Orozco et al., 2006*). At one millimolar divalent cation concentration, PhoQ can be activated by exposure to pH 5.5 or sub-inhibitory concentrations of CAMP (*Bader et al., 2005; Prost et al., 2007*). These are relevant host signals as the macrophage phagosome acidifies to approximately pH 5.5 and contains CAMP (*Alpuche Aranda et al., 1992; Rathman et al., 1996; Rosenberger et al., 2004; Martin-Orozco et al., 2006*). Furthermore, neutralization of acidified macrophage intracellular compartments with chemical inhibitors results in decreased PhoQ-mediated gene expression during infection (*Alpuche Aranda et al., 1992; Martin-Orozco et al., 2006*). Combined, these findings suggested a model in which acidic pH and CAMP activate PhoQ within the macrophage phagosome; however, the individual contribution of these signals to PhoQ-mediated virulence remained unknown.

Acidic pH and CAMP additively activate PhoQ suggesting that the PD has distinct sensing mechanisms for these stimuli (*Prost et al., 2007*). A variety of experimental data indicate that CAMP directly compete with divalent cations for binding sites within the PhoQ PD acidic patch, leading to a model in which CAMP activates PhoQ by disrupting salt-bridges with the inner membrane (*Bader et al., 2005*). The mechanism by which PhoQ is activated by acidic pH appears to be distinct from CAMP and involves perturbations to a network of residues surrounding H157 within the α/β -core of the PD (*Prost et al., 2007*). In this study, we defined conformational changes that occur within the PhoQ PD on exposure to acidic pH. Characterization of the conformational changes induced by acidic pH inspired the construction of PhoQ variants which are impaired for acidic pH and divalent cation sensing, but retain their ability to respond to CAMP. Prior to this study, it was unclear which signals were important for PhoQ-mediated virulence. Utilizing these PhoQ variants, we have now established that acidic pH and divalent cation sensing are dispensable signals for PhoQ-mediated systemic virulence of *Salmonella enterica* Typhimurium, suggesting that CAMP or other host molecules facilitate PhoQ-dependent pathogenesis.

Results

Residues in the PhoQ PD that are dynamic during pH-titration localize proximal to the interface between α -helices 4 and 5 and the α/β -core

PhoQ is activated in acidic conditions in vitro and within the acidified environment of the *Salmonella*-containing vacuole (SCV) after phagocytosis (*Alpuche Aranda et al., 1992; Martin-Orozco et al., 2006; Prost et al., 2007*). However, the mechanism by which the PhoQ PD senses acidic pH is not well characterized. Previously, we reported that the (^1H , ^{15}N)-HSQC-NMR spectrum of the *S. enterica* Typhimurium PhoQ PD is highly sensitive to changes in pH (*Prost et al., 2007*). Therefore, to further understand PhoQ dynamics during activation by acidic pH we collected a series of (^1H , ^{15}N)-HSQC-NMR spectra of the PhoQ PD as a function of pH (**Figure 1A**). To extract residue information from the spectra, resonance assignments were determined for the PhoQ PD at pH 3.5, the condition that yielded the greatest number of observable resonances. Of the 138 residues that can yield HSQC signals, 120 resonances could be assigned in the spectrum at pH 3.5 (**Figure 1B**). The remarkably well dispersed spectrum indicates that the PD remains stably folded, even at pH of 3.5.

In the absence of other pH-dependent processes, resonances that arise from residues that undergo a protonation/deprotonation event will shift in a continuous manner. Such processes will appear in the so-called 'fast-exchange' NMR regime due to the rapid on/off rate of protons. Many resonances in the PD spectra exhibited pH-dependent fast-exchange behavior, consistent with ionization of the many histidine and acidic residues. In addition, some resonances broadened and disappeared from the spectrum as a function of pH. This behavior corresponds to intermediate-to-slow exchange and is indicative of a conformational change or the existence of multiple states that interconvert slowly. Thus, pH-dependent changes in the PhoQ PD HSQC spectra reveal regions of the domain that experience changes in functional group ionization and conformational dynamics.

Spectra, collected at pH 3.5 and pH 6.5, were compared to identify regions in the PhoQ PD that are sensitive to changes in pH (**Figure 2A**). Resonances that experienced significant pH-dependent chemical shift perturbations (CSPs > 0.08 ppm) or broadened beyond detection, localize to regions of the protein that contain ionizable functional groups and/or experience conformational dynamics; thereby defining pH-responsive regions in the domain. Of the 120 assigned residues in the PhoQ PD, resonances from 42 residues were affected by transition from pH 6.5 to 3.5 (**Figure 2B**). Due to resonance overlap and broadening, it is difficult to partition the two spectroscopic effects throughout

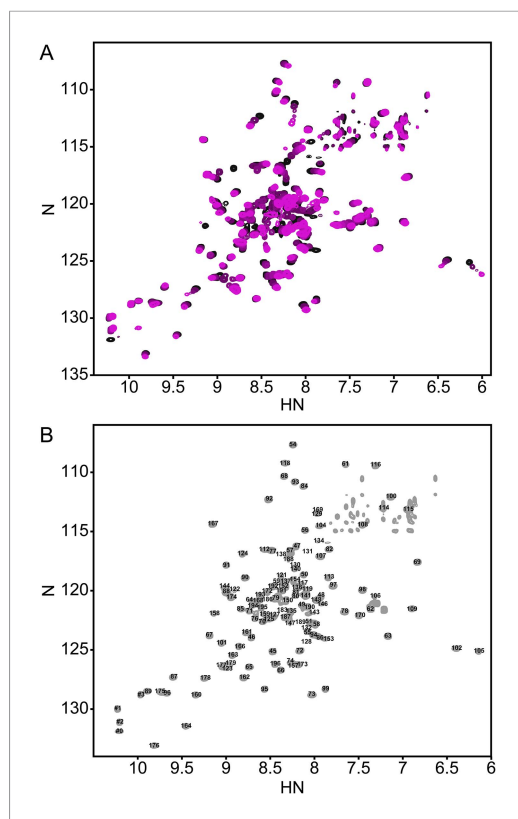


Figure 1. The annotated PhoQ PD (¹H, ¹⁵N)-HSQC-NMR spectrum reveals significant peak shifting and broadening during pH titration. **(A)** (¹H, ¹⁵N)-HSQC-NMR spectra of neutral to acidic pH-titration of the PhoQ PD. The pH-titration is represented as a magenta (pH 6.5) to black (pH 3.5) color gradient. The pH-titration spectra include pH 6.5, 6.0, 5.5, 4.9, 4.1, and 3.5. **(B)** The assigned (¹H, ¹⁵N)-HSQC-NMR spectra of the *S. enterica* Typhimurium PhoQ PD at pH 3.5. Residue numbers are labeled proximal to their corresponding peak.
DOI: [10.7554/eLife.06792.003](https://doi.org/10.7554/eLife.06792.003)

the comparison. Approximately, 20 affected resonances broadened beyond detection at pH 6.5, consistent with pH-dependent conformational dynamics in the PhoQ PD. Furthermore, 66 resonances were relatively unaffected, indicating that the PhoQ PD has pH-insensitive regions.

Assignments for the HSQC spectrum allowed us to identify residues in the PhoQ PD structure that experience pH-dependent changes (**Figure 2C**). A majority of residues affected by pH localize to α 1, α 2, α 4, and α 5 and proximal regions, including β 5, β 6, and β 7. As an independent approach, we randomly mutagenized the PD to identify mutations that activate PhoQ in the presence of repressing concentrations of divalent cations (**Figure 2—figure supplement 1**). pH-sensitive regions identified in the NMR experiments overlap or are proximal to many of the mutations identified in our screen for activating mutations in the PhoQ PD (**Figure 2B**, asterisks). Similar to the activating mutations, a majority of the pH-sensitive residues form an interconnected network which spans α 4 and α 5 and the α/β -core (**Figure 2D**). These data suggested that PhoQ PD residues and structural features important for activation and repression undergo conformational change during pH titration. A majority of the residues that were unaffected by changes in pH mapped distally to α 4 and α 5, providing support for the hypothesis that the detection and response to pH is contained within localized structural elements of the PD. Altogether, these observations are consistent with a model where fluctuations in pH promote local conformational dynamics between α 4 and α 5 and the α/β -core as part of the pH sensing mechanism.

A disulfide bond between α -helices 2 and 4 within the PhoQ PD inhibits activation by acidic pH and divalent cation limitation, but does not restrict activation by CAMP

The NMR and mutagenesis data suggested that α 4 and α 5 are dynamic and that the relationship between the two helices and the α/β -core of the PD likely plays a role in activation. To test this hypothesis, we engineered a PhoQ PD mutant that contains an internal disulfide bond predicted to restrict conformational dynamics between α 4 and α 5 and the α/β -core. Cysteine residues were introduced at positions W104 (on α 2) and A128 (on α 4) based on their side-chain surface exposure, relative geometries, and C β distance (\sim 6 Å) observed in the *S. enterica* Typhimurium PhoQ PD structure (PDB 1YAX). Non-reducing SDS-PAGE and western blotting of membranes harvested from *phoQ*^{W104C-A128C} *S. enterica* Typhimurium revealed a faster migrating PhoQ species relative to wild type, suggesting W104C and A128C form an intramolecular disulfide bond when expressed in bacteria (**Figure 3—figure supplement 1A**). When treated with sample buffer supplemented with β -mercaptoethanol to reduce the disulfide bond, PhoQ^{W104C A128C} migrated similarly to the wild-type protein. Membranes harvested from *phoQ*^{W104C-A128C} *S. enterica* Typhimurium grown in N-minimal media (N-mm) at pH 7.5 or pH 5.5, supplemented with 10 micromolar or 1 millimolar

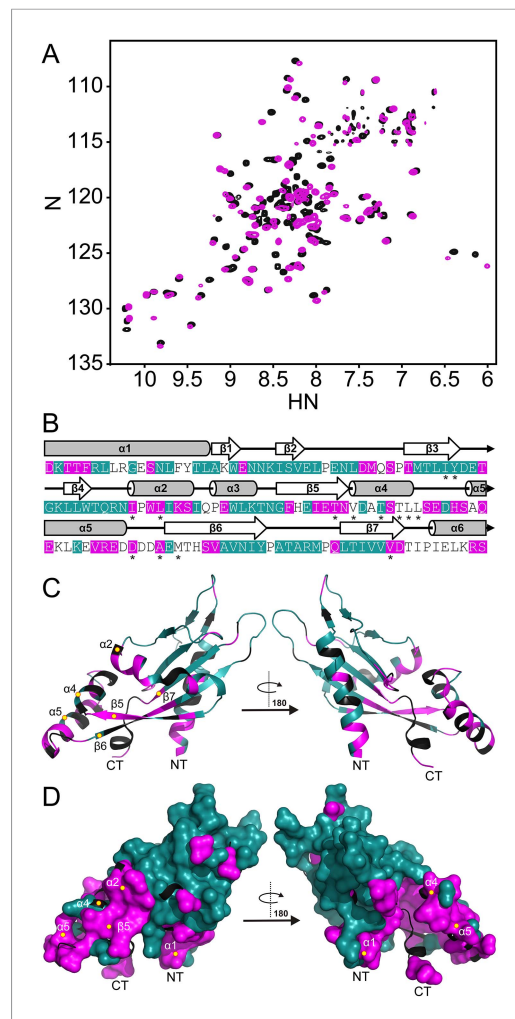


Figure 2. The PhoQ PD experiences significant pH-dependent perturbations which map to $\alpha 4$ and $\alpha 5$ and the α/β -core. **(A)** Comparison of $(^1\text{H}, ^{15}\text{N})$ -HSQC-NMR spectra of the PhoQ PD at pH 6.5 (magenta) and pH 3.5 (black). **(B)** Residues that experience CSPs >0.08 ppm and/or peak broadening determined from the spectral comparison in panel **A** are mapped onto the *S. enterica* Typhimurium PhoQ PD (residues 45–188) primary and secondary structures (pH-sensitive residues, magenta; pH-insensitive residues, teal; ambiguous or non-assigned residues, no color). The locations of activating mutations from **Figure 2—figure supplement 1** are indicated with asterisks. **(C)** pH-sensitive residues from panel **A** mapped onto the PhoQ PD structure (PDB 1YAX); pH-sensitive residues (magenta), pH-insensitive residues (teal), and ambiguous or non-assigned residues (black). pH-sensitive secondary structural features are labeled with yellow circles (NT, N-termini; CT, C-termini). **(D)** Continuous surface representation (1.4 Å probe) of pH-sensitive (magenta) and pH-insensitive (teal) residues from panel **C** mapped onto the PhoQ PD crystal structure.

DOI: 10.7554/eLife.06792.004

The following figure supplement is available for figure 2:

Figure 2. continued on next page

MgCl_2 , or CAMP showed no observable differences in PhoQ^{W104C-A128C} disulfide bond formation by SDS-PAGE, suggesting formation of the W104C-A128C disulfide bond is not dependent on growth conditions or PhoQ activation state (data not shown). These data indicated that the disulfide bond formed between W104C-A128C is stably maintained within the *S. enterica* Typhimurium periplasm.

The PhoQ^{W104C-A128C} disulfide mutant was designed to inhibit motion between $\alpha 2$ and $\alpha 4$, allowing us to determine whether the dynamics of $\alpha 4$ and $\alpha 5$ play a critical role in activation. When exposed to acidic pH or low divalent cation growth media, activation of the PhoQ-dependent *phoN::TnphoA* reporter in *S. enterica* Typhimurium was significantly reduced in *phoQ*^{W104C-A128C} relative to wild type (**Figure 3A**). Additionally, the previously identified T48I activating mutation in the T48 D179 K186 (TDK) network in the PhoQ PD (Miller and Mekalanos, 1990; Garcia Vescovi et al., 1996; Sanowar et al., 2003; Cho et al., 2006) was suppressed by the W104C-A128C disulfide bond, supporting the hypothesis that $\alpha 4$ and $\alpha 5$ and the TDK network are an interconnected signaling element (**Figure 3B**). Interestingly, the T48I mutation potentiates CAMP activation in the *phoQ*^{T48I W104C-A128C} background by an unknown mechanism. Importantly, CAMP still activated the *phoN::TnphoA* reporter in *phoQ*^{W104C-A128C} and *phoQ*^{T48I W104C-A128C} *S. enterica* Typhimurium at or above wild-type levels, indicating that these mutant proteins are functional (**Figure 3A,B**). Chromosomal *phoQ*^{W104C-A128C} had a similar phenotype to *phoQ*^{W104C-A128C} expressed from the pBAD24 vector, indicating the phenotype is not an artifact of expression *in trans* (**Figure 3—figure supplement 1B**). Furthermore, the *phoQ*^{W104C-A128C} phenotype does not appear to be exclusive to *phoN* as other PhoQ-regulated genes—*pagD*, *pagO*, and *phoP*—are significantly reduced for induction by acidic pH and divalent cation limitation, but are induced by exposure to CAMP, similar to wild-type bacteria (**Figure 3—figure supplement 2**). Serine substitutions at W104 and A128 did not recapitulate the phenotype observed for *phoQ*^{W104C-A128C}, but rather resulted in increased *phoN::TnphoA* reporter activity relative to wild type (**Figure 3—figure supplement 1C**). Additionally, neither single cysteine nor single serine substitutions at W104 or A128 recapitulated the *phoQ*^{W104C-A128C} phenotype (**Figure 3—figure supplement 1D**). These results confirmed that a disulfide bond is required for the *phoQ*^{W104C-A128C}

Figure 2. Continued

Figure supplement 1. Residues involved in PhoQ activation and repression form a buried network connecting $\alpha 4$ and $\alpha 5$ to the α/β -core.

DOI: [10.7554/eLife.06792.005](https://doi.org/10.7554/eLife.06792.005)

inhibits activation by acidic pH, divalent cation limitation, and activating mutations in the TDK network. These data suggest that CAMP activates PhoQ by a mechanism that is distinct and separable from the mechanism by which acidic pH or divalent cation limitation activate PhoQ.

The PhoQ^{W104C-A128C} PD is structurally similar to wild type and has increased stability

A disulfide bond spanning helices $\alpha 2$ and $\alpha 4$ inhibits activation of PhoQ^{W104C-A128C} by acidic pH and divalent cation limitation. Given the remarkable phenotype of this mutant, we sought to ascertain whether the PhoQ^{W104C-A128C} PD maintains a similar structure to the wild-type PD. A crystal structure of the *S. enterica* Typhimurium PhoQ^{W104C-A128C} PD (PDB 4UEY) was solved at 1.9 Å resolution (Figure 4A and Table 1). As predicted, the PhoQ^{W104C-A128C} PD formed an intramolecular disulfide bond between W104C and A128C, covalently linking $\alpha 2$ and $\alpha 4$ (Figure 4A, inset). The protomers in the PhoQ^{W104C-A128C} PD structure are highly similar to each other, with an average root mean squared deviation (r.m.s.d.) of 0.3. Furthermore, the disulfide mutant structure is similar to previously solved structures of wild-type *S. enterica* Typhimurium (PDB 1YAX) and *Escherichia coli* (PDB 3BQ8) PhoQ PD, with an average r.m.s.d. value of 1.07 Å (Figure 4B). These data further demonstrate that the PhoQ^{W104C-A128C} PD forms an intramolecular disulfide bond and a structure similar to the wild-type PhoQ PD.

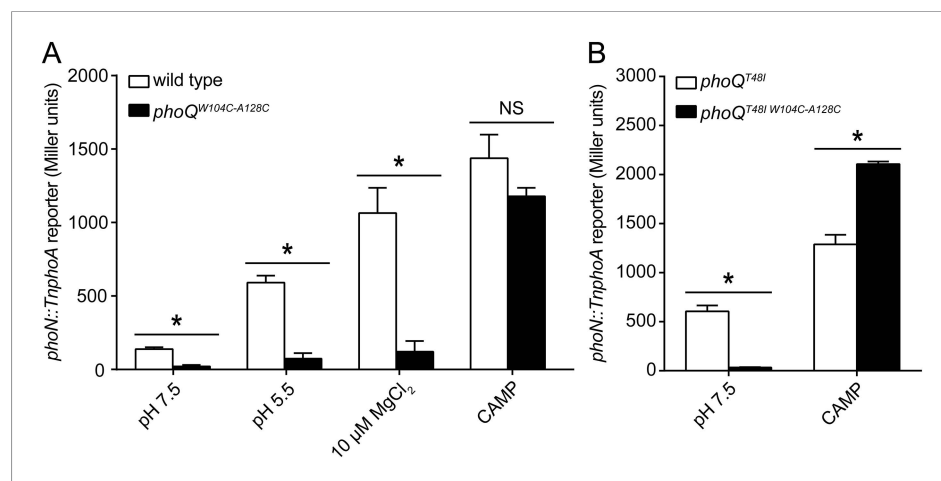


Figure 3. A disulfide bond between α -helices 2 and 4 inhibits PhoQ activation by acidic pH and divalent cation limitation, but does not inhibit activation by CAMP. PhoQ-dependent *phoN::TnpHoA* alkaline phosphatase activity of (A) wild-type and *phoQ*^{W104C-A128C} or (B) *phoQ*^{T48I} and *phoQ*^{T48I W104C-A128C} *S. enterica* Typhimurium strains grown in basal (pH 7.5) or activating (pH 5.5, 10 μ M MgCl₂, or CAMP) N-mm. (A and B) The data shown are representatives from at least three independent experiments performed in duplicate and presented as the mean \pm SD. Unpaired Student's t-test was performed between wild type and *phoQ*^{W104C-A128C} or *phoQ*^{T48I} and *phoQ*^{T48I W104C-A128C} for all conditions; (*) p \leq 0.05, (NS) not significantly different.

DOI: [10.7554/eLife.06792.006](https://doi.org/10.7554/eLife.06792.006)

The following figure supplements are available for figure 3:

Figure supplement 1. The PhoQ^{W104C-A128C} disulfide forms in the *Salmonella* periplasm and individual mutations at W104 or A128 do not inhibit activation by acidic pH or divalent cation limitation.

DOI: [10.7554/eLife.06792.007](https://doi.org/10.7554/eLife.06792.007)

Figure supplement 2. Multiple PhoQ-dependent genes in *phoQ*^{W104C-A128C} *Salmonella* are induced by CAMP, but not by acidic pH or divalent cation limitation.

DOI: [10.7554/eLife.06792.008](https://doi.org/10.7554/eLife.06792.008)

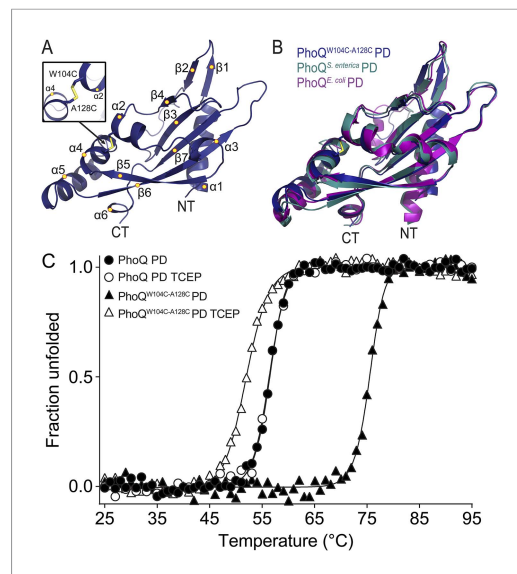


Figure 4. The PhoQ^{W104C-A128C} PD is structurally similar to wild type and has increased stability. **(A)** 1.9 Å crystal structure of the *S. enterica* Typhimurium PhoQ^{W104C-A128C} PD (PDB 4UEY). The W104C-A128C disulfide bond (inset) is located between α2 and α4. Secondary structural features are annotated with yellow circles (NT, N-termini; CT, C-termini). **(B)** Structural comparison of the PhoQ^{W104C-A128C} PD (blue), the wild-type *S. enterica* Typhimurium PhoQ PD (PDB 1YAX, teal), and the wild-type *E. coli* PhoQ PD (PDB 3BQ8, purple). **(C)** Thermal denaturation of wild-type *S. enterica* Typhimurium PhoQ PD and PhoQ^{W104C-A128C} PD treated with or without TCEP reducing agent monitored by CD spectroscopy at 212 nm. Raw data were normalized to give the fraction unfolded protein assuming a two-state denaturation process. A sigmoidal curve was fit to the processed data. The data shown are representatives from three independent experiments.

DOI: [10.7554/eLife.06792.009](https://doi.org/10.7554/eLife.06792.009)

The following figure supplement is available for figure 4:

Figure supplement 1. Wild-type and PhoQ^{W104C-A128C} PD have similar secondary structure.
DOI: [10.7554/eLife.06792.010](https://doi.org/10.7554/eLife.06792.010)

We hypothesize that the W104C-A128C disulfide may stabilize conformational dynamics between α4 and α5 and the α/β-core, preventing acidic pH from promoting a flexible, active state. This hypothesis was tested by performing thermal melts on purified PhoQ PD and PhoQ^{W104C-A128C} PD at pH 5.5 by following the CD signal of each protein as a function of temperature. We first confirmed that purified PhoQ^{W104C-A128C} PD forms a disulfide as visualized as a shift in SDS-PAGE migration rate relative to PhoQ PD and TCEP-reduced PhoQ^{W104C-A128C} (Figure 4—figure supplement 1A). The CD spectra revealed that the PhoQ PD and PhoQ^{W104C-A128C} PD with or without TCEP are folded and have relatively similar secondary structure at pH 5.5 and 25°C (Figure 4—figure supplement 1B). Thermal denaturation of the PhoQ PD at pH 5.5 proved to be irreversible. Therefore, we reported the apparent transition temperatures (T_m^{app}). While the wild-type PhoQ PD unfolded with a T_m^{app} of 56°C in the presence and absence of TCEP (Figure 4C), the PhoQ^{W104C-A128C} PD had a significantly increased T_m^{app} of 75°C. When reduced with TCEP, the PhoQ^{W104C-A128C} PD was slightly destabilized relative to the wild type, with a T_m^{app} 52°C. Therefore, the W104C-A128C disulfide increased the intrinsic stability of the PD at pH 5.5 relative to wild type. Furthermore, the observations that reduced PhoQ^{W104C-A128C} PD is less stable than wild type and that *phoQ*^{W104C-A128C} bacteria had increased PhoQ-dependent gene reporter activity relative to wild type (Figure 3—figure supplement 1C) suggests that substituting small polar side-chains at these positions in the PD results in decreased stability and increased PhoQ activity. Combined, these results suggest that the mechanism by which the W104C-A128C disulfide bond inhibits PhoQ activation by acidic pH and divalent cation limitation involves a loss of conformational flexibility between α4 and α5 and the α/β-core.

***Salmonella* strains with the *phoQ*^{W104C-A128C} allele are competent for survival during systemic virulence in mice and within cultured macrophage**

Prior to this study, the contribution of specific stimuli to PhoQ-mediated bacterial virulence was difficult to ascertain as mutants that only respond to individual signals were not available. With the construction of *phoQ*^{W104C-A128C} *S. enterica* Typhimurium, the significance of acidic pH and divalent cation sensing by PhoQ to virulence could be directly determined independently of CAMP sensing. Thus, BALB/c mice were infected by the intraperitoneal (IP) route with wild-type, *phoQ*^{W104C-A128C}, or *phoQ* null (Δ *phoQ*) bacteria and splenic bacterial burden was determined at 48- and 96-hpi (Figure 5A, solid lines). Similar to infection with wild-type bacteria, mice infected with *phoQ*^{W104C-A128C} bacteria had increased splenic bacterial burden relative to those infected with Δ *phoQ* bacteria. The equivalent experiment was performed in resistant A/J mice to determine if the virulence phenotype observed for mice infected with *phoQ*^{W104C-A128C} bacteria was due to the susceptible BALB/c mouse

Table 1. Crystallographic data collection and refinement

PhoQ^{W104C-A128C} PD	
Data collection	
Space group	C2
Cell dimensions	
<i>a</i> , <i>b</i> , <i>c</i> (Å)	128.04, 45.37, 81.37
α , β , γ (°)	90, 102.53, 90
Resolution (Å)	31.3–1.9 (2.01–1.90)*
R_{sym} or R_{merge}	0.05 (0.51)
$I/\sigma I$	12.9 (1.6)
Completeness (%)	97.8 (93.8)
Redundancy	3.6 (3.2)
Refinement	
Resolution (Å)	31.3–1.90 (1.95–1.90)*
No. reflections	35,633
$R_{\text{work}}/R_{\text{free}}$	0.23/0.26 (0.38/0.44)
No. atoms (all)	
Protein	3391
Water	138
Ca ²⁺	–
<i>B</i> -factors	
Protein	44.8
Water	40.6
R.m.s. deviations	
Bond lengths (Å)	0.007
Bond angles (°)	1.2
Ramachandran statistics	
Residues in favored region no (%)	409 (98.3)
Residues in allowed region no (%)	7 (1.7)
Residues in outlier region no (%)	0 (0)
PDB-entry	4UEY
Crystallization conditions	0.1 M Bis-Tris pH 6.5, 200 mM MgCl ₂ , 25% Peg3350

*Values in parentheses are for highest-resolution shell.

DOI: [10.7554/eLife.06792.011](https://doi.org/10.7554/eLife.06792.011)

genetic background and to determine whether a subtle fitness defect would be exposed on infection of a relatively resistant inbred mice. Infecting A/J mice revealed the same relative phenotypes for wild-type, *phoQ*^{W104C-A128C}, and Δ *phoQ* bacteria, although, as expected, bacterial burden was lower compared to infected BALB/c mice (**Figure 5A**, dotted lines). These results indicate that PhoQ sensing of acidic pH and divalent cation limitation are dispensable for systemic virulence of *S. enterica* Typhimurium in susceptible and relatively resistant inbred mice.

The importance of PhoQ activation by acidic pH and divalent cation limitation for systemic infection was also assessed by competing *phoQ*^{W104C-A128C} bacteria with wild-type *S. enterica* Typhimurium in IP or peroral (PO) infections of BALB/c mice. The splenic bacterial competitive index (CI) for wild-type, *phoQ*^{W104C-A128C}, and Δ *phoQ* bacteria was determined for both IP and PO infections at 48-hpi or 96-hpi, respectively (**Figure 5B** and **Figure 5—figure supplement 1**). Consistent with the single strain infections, *phoQ*^{W104C-A128C} demonstrated no reduction in CI and, in contrast, was more competitive than wild type. Δ *phoQ* showed the expected reduction in CI. Altogether, these data indicate that

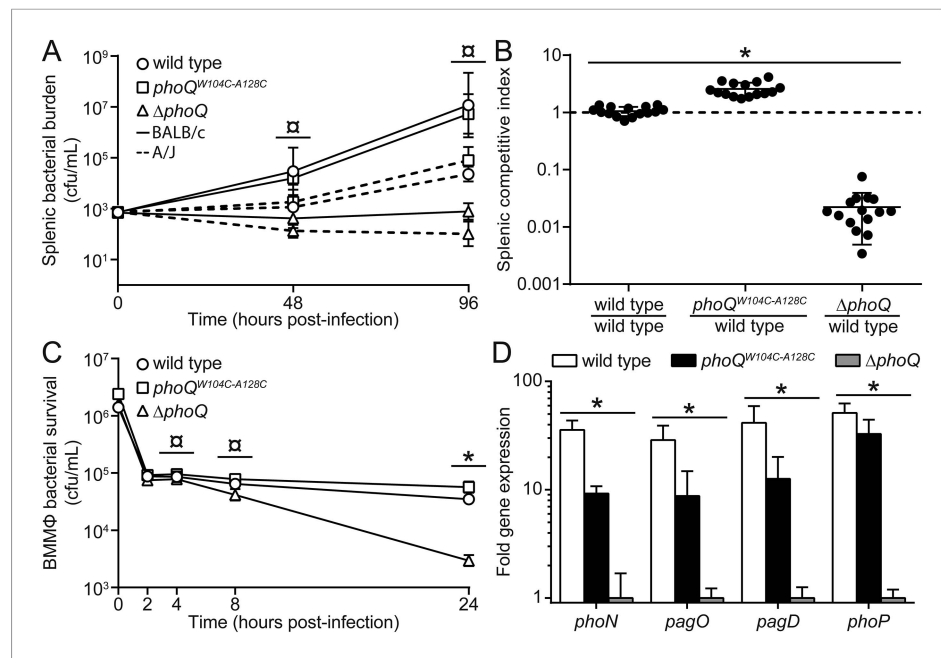


Figure 5. *phoQ*^{W104C-A128C} *Salmonella* survive within host organisms and exhibits PhoQ-dependent gene expression within macrophage. **(A)** Individual *S. enterica* Typhimurium strains administered IP to BALB/c (solid lines) or A/J (dotted lines) mice. The inoculum is shown at T = 0 hpi. Spleens were harvested and bacterial burden quantified. **(B)** Competition between *S. enterica* Typhimurium strains administered IP to BALB/c mice. Spleens were harvested, bacteria quantified 48-hpi and CI determined. **(A and B)** The data shown are representatives from at least three independent experiments performed in quintuplet and presented as the mean \pm SD. **(C)** BALB/c BMM Φ infected with strains of *S. enterica* Typhimurium. Bacteria were harvested and quantified at the indicated time-points. The inoculum is shown at T = 0 hpi. The data shown are representatives from at least three independent experiments performed in triplicate and presented as the mean \pm SD. **(D)** PhoQ-dependent gene expression from *S. enterica* Typhimurium strains within BALB/c BMM Φ 4-hpi. Gene expression was normalized to *rpoD* and presented as fold-induction relative to Δ *phoQ*. The data shown are representatives from at least three independent experiments and presented as the mean \pm SD. **(A, B, C, and D)** Unpaired Student's *t*-test was performed between all strains (bar) for each time-point or gene. Symbols for significant difference; (α) wild type and *phoQ*^{W104C-A128C} are not significantly different from each other ($p \geq 0.05$), but are significantly different from Δ *phoQ* ($p \leq 0.05$), (*) all strains are significantly different from each other ($p \leq 0.05$).

DOI: [10.7554/eLife.06792.012](https://doi.org/10.7554/eLife.06792.012)

The following figure supplements are available for figure 5:

Figure supplement 1. Acidic pH and divalent cation sensing by PhoQ are dispensable for PO systemic competition of *S. enterica* Typhimurium.

DOI: [10.7554/eLife.06792.013](https://doi.org/10.7554/eLife.06792.013)

Figure supplement 2. The in vitro growth rate of wild-type *Salmonella* is decreased relative to *phoQ*^{W104C-A128C} and Δ *phoQ* when grown at pH 5.5.

DOI: [10.7554/eLife.06792.014](https://doi.org/10.7554/eLife.06792.014)

PhoQ activation by acidic pH and divalent cation limitation are dispensable for *S. enterica* Typhimurium to out compete strains with these capabilities during systemic infection of susceptible mice. Furthermore, the observation that IP and PO administered *phoQ*^{W104C-A128C} *S. enterica* Typhimurium have similar competitive indices suggests that acidic pH and divalent cation sensing by PhoQ are not required for survival or spread from the gastrointestinal tract to deep tissue sites.

S. enterica Typhimurium is growth restricted in cultured fibroblasts and nonphagocytic stromal cells in the murine lamina propria via PhoPQ-dependent processes (Cano et al., 2001; Nunez-Hernandez et al., 2013). Thus, it was plausible that the competitive advantage observed for *phoQ*^{W104C-A128C} relative to wild-type bacteria was due to an increased growth rate resulting from the loss of acidic pH sensing by PhoQ. When grown in N-mm pH 5.5, wild-type bacterial growth rate was decreased relative to *phoQ*^{W104C-A128C} and Δ *phoQ* (Figure 5—figure supplement 2). Conversely, wild

type, *phoQ*^{W104C-A128C}, and Δ *phoQ* grown in N-mm pH 7.5 had similar growth kinetics. These data provide evidence that acidic pH sensing by PhoQ reduces *S. enterica* Typhimurium growth rate in vitro and correlates with the in vivo competitive advantage that was observed for *phoQ*^{W104C-A128C} bacteria within mice spleens.

The contribution of acidic pH and divalent cation limitation as signals for PhoQ-mediated bacterial intracellular survival within macrophages was evaluated by measuring *S. enterica* Typhimurium survival after infection of bone-marrow derived macrophages (BMM Φ) from BALB/c mice. BMM Φ were infected with wild-type, *phoQ*^{W104C-A128C}, or Δ *phoQ* *S. enterica* Typhimurium strains and bacterial burden was determined at 2-, 4-, 8-, and 24-hpi (Figure 5C). No difference in bacterial burden was observed between wild type, *phoQ*^{W104C-A128C}, and Δ *phoQ* at 2- or 4-hpi. At 8- and 24-hpi, bacterial burden for Δ *phoQ* was decreased relative to wild type and *phoQ*^{W104C-A128C}. Importantly, bacteria with the *phoQ*^{W104C-A128C} allele maintained at or above wild-type bacterial levels throughout infection. These data indicate that activation of PhoQ by acidic pH and divalent cation limitation are dispensable for *S. enterica* Typhimurium survival within BMM Φ from inbred mice.

PhoQ-dependent gene expression is induced in *phoQ*^{W104C-A128C} *Salmonella* within cultured macrophages

The discovery of the *phoQ*^{W104C-A128C} phenotype allowed for the unique opportunity to examine the contribution of acidic pH and divalent cation sensing to PhoQ-dependent gene expression during infection of macrophages. Therefore, BMM Φ from BALB/c mice were infected with wild-type, *phoQ*^{W104C-A128C}, or Δ *phoQ* *S. enterica* Typhimurium. Following incubation, PhoQ-dependent gene expression was determined for intracellular *S. enterica* Typhimurium (Figure 5D). Wild-type bacteria experienced 41-, 29-, 36-, and 51-fold increases in gene expression for *pagD*, *pagO*, *phoN*, and *phoP*, whereas *phoQ*^{W104C-A128C} experienced increases of 12-, 9-, 9-, and 33-fold, respectively, relative to Δ *phoQ* bacteria. These data may indicate that wild-type acidic pH or divalent cation sensing contribute an approximate threefold to fourfold increase in PhoQ-dependent gene expression relative to *phoQ*^{W104C-A128C}; however, a significant amount of gene expression (\geq ninefold) appeared to be independent of acidic pH or divalent cation sensing. These findings are consistent with in vitro results which show that acidic pH and CAMP are additive signals for PhoQ (Prost et al., 2007). These data indicate that maximal PhoQ-dependent gene expression in macrophages requires acidic pH or divalent cation sensing. Furthermore, these findings reveal that the *phoQ*^{W104C-A128C} allele promotes significant induction of PhoQ-dependent gene expression, suggesting CAMP or alternative host factors, other than acidic pH and divalent cation limitation, are a major signal for *S. enterica* Typhimurium within BMM Φ vacuoles.

Discussion

Salmonellae encounter changing environments within the macrophage phagosome and other mammalian host sites during infection. These environments include a variety of antimicrobial factors for which the bacteria must regulate inducible resistance mechanisms in order to survive. These bacterial resistance mechanisms are essential for successful infection, necessitating tight regulation by sensors such as PhoQ. Our study defines α 4 and α 5 in the PhoQ PD as a pH-responsive structural element that experiences a change in its dynamic behavior upon transition to acidic pH. Furthermore, mutations within the PhoQ PD, predicted to destabilize hydrophobic packing and hydrogen bonding between the α / β -core and α 4 and α 5, resulted in loss of PhoQ repression. Limiting flexibility between these structural elements by introduction of a disulfide bond inhibited PhoQ activation by acidic pH and divalent cation limitation. We suggest that PhoQ has evolved α 4 and α 5 as a unique pH-responsive structural element within the PD, effectively replacing the ligand-binding site that is often found in a similar location in other structurally related PDC sensor domains (Cho et al., 2006; Cheung and Hendrickson, 2008).

This study provides insights for a refined model of PhoQ activation (Figure 6). At neutral pH and millimolar divalent cation concentration (Figure 6, left), the PhoQ PD is anchored to the inner membrane in a repressed state via cation-bridges, a rigid α / β -core and TDK network, and quiescent α 4 and α 5. Acidic pH or divalent cation limitation promotes a change in α 4 and α 5 from a stable to a dynamic state (Figure 6, middle). Acidic pH-induced flexibility in α 4 and α 5 may destabilize divalent cation salt-bridges between the inner membrane and acidic patch, thereby promoting a loss of

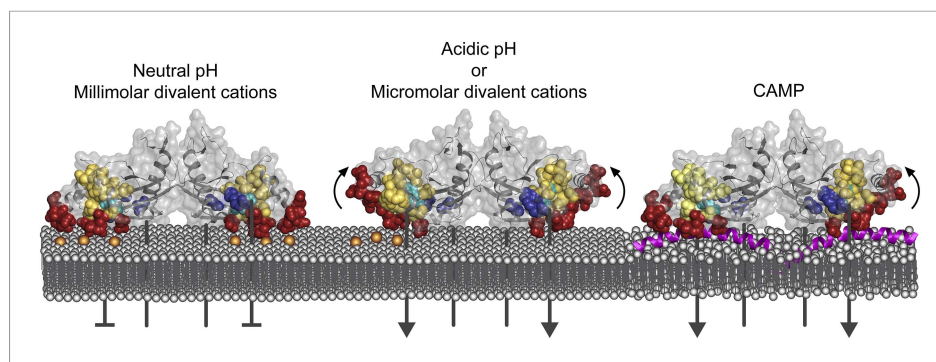


Figure 6. Model of PhoQ activation and repression. (Left) At neutral pH and millimolar divalent cation concentration, the PhoQ PD is maintained in a repressed conformation due to rigidified interactions between the α/β -core (yellow spheres), $\alpha 4$ and $\alpha 5$, and salt-bridges (bronze spheres) formed between the acidic patch (red spheres) and inner membrane. (Middle) Transition to a mildly acidic (left protomer) or divalent cation limited (right protomer) environment promotes flexibility in $\alpha 4$ and $\alpha 5$ (bent arrows) and conformational dynamics in the α/β -core surrounding H157 (teal spheres). Movement in $\alpha 4$ and $\alpha 5$ due to acidic pH or divalent cation limitation destabilizes salt-bridges between the acidic patch and inner membrane perturbing the TDK network (blue spheres) resulting in activation. (Right) CAMP (magenta helices) intercalates into the inner membrane and promotes PhoQ activation by directly interacting with the PhoQ transmembrane domains and/or by disrupting local phospholipid packing (left protomer) and/or by overcoming constraints in $\alpha 4$ and $\alpha 5$ (right monomer, bent arrow).

DOI: [10.7554/eLife.06792.015](https://doi.org/10.7554/eLife.06792.015)

divalent cation-mediated repression. Lack of divalent cation salt-bridges between the PhoQ PD acidic patch and inner membrane due to divalent cation limitation may result in electrostatic repulsion between the acidic patch and inner membrane, releasing $\alpha 4$ and $\alpha 5$, and favoring a more flexible state in this structural element. Changes in the relationship between $\alpha 4$ and $\alpha 5$ and the α/β -core surrounding H157 are transmitted to the dimerization interface and TDK network proximal to the membrane resulting in alterations of the transmembrane domain, cytoplasmic HAMP domain, and ultimately resulting in increased PhoQ kinase activity.

Our model of PhoQ activation and repression has similarities to a recently proposed two-state computational model in which the PD is predicted to experience broad conformational changes within the periplasmic dimerization interface and acidic patch (Molnar et al., 2014). This model is consistent with predictions previously made in relation to the discovery of the divalent cation bridges between the PhoQ acidic patch and negatively charged membrane phospholipids (Bader et al., 2005; Cho et al., 2006). Molnar et al suggest that the PhoQ PD assumes alternative conformations as the acidic patch moves away from the membrane in the absence of divalent cation. Our findings that restricting movement in $\alpha 4$ and $\alpha 5$ inhibits PhoQ activation by acidic pH and divalent cation limitation supports the model that the acidic patch and $\alpha 4$ and $\alpha 5$ must remain dynamic for proper signaling. Furthermore, our observations that PhoQ activation by acidic pH and divalent cation limitation are separable from CAMP-mediated activation may indicate that distinct conformational states exist for each of the unique PhoQ-activating and -repressing stimuli.

Results presented here indicate that $\alpha 4$ and $\alpha 5$ within the PhoQ PD do not adopt a distinct conformation under activating pH conditions, but rather exchange between a rigid, repressed state and an ensemble of conformations that together constitute the acidic pH-activated state. Unlike other pH-sensors that utilize discrete histidine protonation as a mechanism of activation (Perier et al., 2007; Dawson et al., 2009; Müller et al., 2009; Choi et al., 2013; Williamson et al., 2013), PhoQ activation by acidic pH does not appear to rely strictly on protonation of histidines. Mutagenesis of H157, which is located in the PhoQ PD α/β -core and is observed to form hydrogen bonds with T129 on $\alpha 4$ and the backbone hydroxyl of T180 on the $\beta 7$ - $\alpha 6$ loop, results in a modest increase in activity; however, it does not account for the entire pH-mediated activation state (Prost et al., 2007). Mutation of the other two histidines in the PD (H137 and H120) did not significantly affect activation or repression of PhoQ (data not shown). An alternate mechanism of PhoQ activation by acidic pH may involve pH-induced conformational changes within the periplasmic dimerization interface. Notably, an intermolecular disulfide at position T61C in the PhoQ PD dimerization interface results in increased PhoQ-dependent

reporter activity at pH 5.5, suggesting that conformational changes in the dimerization interface can directly affect signal transduction (data not shown). Furthermore, analytical ultracentrifugation analysis revealed that the PhoQ PD dimer dissociates as the pH decreases (data not shown). Additionally, work by Molnar et al support the notion that conformational changes with the dimerization interface are concomitant with activation and repression. Recently, it was shown that the *Helicobacter pylori* chemotaxis receptor, TlpB, utilizes a unique mechanism to sense acidic pH (**Goers Sweeney et al., 2012**). Interestingly, the TlpB PD may sense pH by adopting a 'relaxed' conformation at low pH due to decreased hydrogen bonding to a coordinated urea molecule. It is plausible that similar relaxation may occur in the PhoQ PD between the α/β -core and helices $\alpha 4$ and $\alpha 5$ upon exposure to acidic pH. Therefore, pH-induced conformational changes resulting in structural relaxation or flexibility may be an important mechanism by which pH can be sensed.

Our previous work suggests that PhoQ activation by acidic pH and CAMP proceed via different mechanisms (**Bader et al., 2005; Prost et al., 2007**). In this study, we have shown that activation by acidic pH and divalent cation limitation are separable from CAMP-mediated activation by rigidifying the interaction between $\alpha 4$ and $\alpha 5$ and the α/β -core. Perhaps, CAMP circumvents $\alpha 4$ and $\alpha 5$ and activates PhoQ via direct interactions within the transmembrane regions adjacent to the acidic patch or disrupts local phospholipid packing promoting conformational changes in the periplasmic and transmembrane domains (**Figure 6**, right). Alternatively, it is plausible that CAMP functions as a large steric 'wedge'. In this scenario, CAMP is recruited to the acidic patch of PhoQ resulting in conformational changes in the PD overcoming any repressive structural constraints between $\alpha 4$ and $\alpha 5$ and the α/β -core.

Determining the host signals which activate PhoQ has been difficult; past investigations have relied on alterations to host processes via chemical inhibitors to neutralize acidic compartments or targeted mutagenesis to remove known PhoQ-activating antimicrobial peptides from host animals (**Alpuche Aranda et al., 1992; Martin-Orozco et al., 2006; Richards et al., 2012**). Although informative, these studies do not account for unintended host-cell changes due to chemical neutralization of acidic vesicles and organelles or uncharacterized host peptides or molecules which may activate the system. For example, distinct pH-gradients are established and required in eukaryotic vesicular trafficking pathways and chemical neutralization of acidic compartments within these pathways results in a variety of cellular disturbances including inhibition of acidic hydrolases and proteases, perturbation of molecular sorting and recycling, endocytosis and exocytosis dysregulation, and disruption of vesicular fusion events (**Dean et al., 1984; Mellman et al., 1986; Casey et al., 2010**). Furthermore, chemical neutralization of the SCV is detrimental to intracellular *S. enterica* Typhimurium as it results in decreased bacterial survival (**Rathman et al., 1996**), presumably due to lack of virulence factor expression. Therefore, it is plausible that the use of chemical inhibitors to block or neutralize acidic host-compartments inhibits processes involved in CAMP maturation or trafficking, thereby preventing activation of PhoQ.

It is plausible that undefined host molecules or conditions, that require defined pH-gradients, activate PhoQ in vivo. Our observations that activation by acidic pH and divalent cation limitation are not required for significant increases in PhoQ-dependent gene expression in BALB/c macrophage and that PhoQ-dependent gene expression is induced in CRAMP-deficient macrophage (**Richards et al., 2012**) indicate that uncharacterized host factors, which are likely to be a variety of different cationic antimicrobial molecules, activate PhoQ. Furthermore, multiple host peptides may activate PhoQ in vivo as various host and synthetically derived cationic peptides can activate the system; this is consistent with the large PhoQ PD acidic patch which likely evolved to bind diverse CAMP (**Bader et al., 2003, 2005; Shprung et al., 2012**). From these observations, it is reasonable to speculate that the acidic patch, located on the $\alpha 4/\alpha 5$ structural unit within the PhoQ PD of bacteria that interact with animals, evolved to sense a variety of cationic peptides, as the PhoQ PD from environmental bacteria such as *Pseudomonas aeruginosa* lack these important structural features (**Prost et al., 2008**).

Though it is tempting to speculate that CAMP may be the dominant PhoQ-stimulant during systemic infection, it is important to remember that sensing may be redundant or host-compartment specific. Further experiments will need to be performed to examine the contribution of acidic pH and divalent cation sensing to PhoQ-mediated bacterial survival during transition from the intestinal tract to systemic environments and determine if 'bacterial innate immunity' or the recognition of multiple mammalian signals is redundant. Additionally, perhaps acidic pH and divalent cation sensing by PhoQ are functions required for survival in ex vivo environments, beyond animal hosts.

The work in this study led to the construction of a specific *S. enterica* Typhimurium PhoQ mutant that is inhibited for activation by acidic pH or divalent cation limitation. This mutant has wild-type virulence in susceptible and resistant mouse models of systemic infection suggesting that, at least in these models, acidic pH and divalent cation sensing are dispensable for virulence. Although we have shown that the PhoQ^{W104C-A128C} disulfide forms in purified proteins and in bacteria grown in culture, we did not measure disulfide formation for W104C-A128C within host tissues. Host compartments replete with strong oxidizing agents, such as the macrophage phagosome, could potentially disrupt disulfide bond formation. However, multiple *Salmonella* virulence factors and homeostatic processes that occur in the macrophage phagosome require disulfide bond formation, indicating that *S. enterica* has robust mechanisms to regulate redox potential and resist hyperoxidation of thiols in the periplasm (Ellermeier and Schlauch, 2004; Miki et al., 2004; Lipka and Goulian, 2012). Additionally, we have observed altered PhoQ-dependent gene expression from *phoQ*^{W104C-A128C} *S. enterica* Typhimurium within macrophage phagosomes similar to in vitro grown bacteria. Therefore, it is highly likely that efficient formation of the W104C-A128C disulfide bond occurs inside host compartments.

In summary, we provide novel detail to the mechanism by which *S. enterica* Typhimurium PhoQ is activated by acidic pH. We have identified residues and secondary structural elements within the PD which contribute to acidic pH sensing and are important for PhoQ signal transduction. Furthermore, structural studies have led to the engineered bifurcation of PhoQ signaling capabilities; separating acidic pH and divalent cation sensing from CAMP signaling. This discovery has allowed us to determine the contribution of acidic pH and divalent cation sensing to *S. enterica* Typhimurium virulence and will provide valuable insights to the spatial-temporal regulation of PhoQ during pathogenesis.

Materials and methods

Bacterial strains and growth conditions

Bacterial strains, plasmids, and primers used in this study can be found in **Tables 2, 3**. *S. enterica* Typhimurium strain 14028s was the wild-type strain used in this study and all subsequent strains and mutants were derived from this strain. Unless otherwise stated, all alkaline phosphatase activity assays were performed in the CS1081 background with CS1084 as the wild-type control and various alleles of *phoQ* basally expressed from pBAD24. Alkaline phosphatase activity assays were also performed on wild type (KH127) and *phoQ*^{W104C-A128C} (KH130) recombined on to the chromosome of CS1081. Bacterial strains were grown in either LB broth or modified N-mm as indicated. Activation of the *phoN::TnphoA* reporter was utilized as previously described (Bader et al., 2005; Prost et al., 2007). Briefly, bacterial strains were grown overnight in modified N-minimal media pH 7.5 containing 1 mM MgCl₂. In the morning, cultures were washed once in the appropriate media and diluted 1:100 in to fresh modified N-minimal media containing either 10 μM, 1 mM, or 10 mM MgCl₂ and buffered with either 0.1 M Tris or 0.1 M MES to pH 7.5 or pH 5.5, respectively. Unless stated otherwise, the base growth media is N-minimal media pH 7.5 supplemented with 1 mM MgCl₂ and 100 μg•ml⁻¹ ampicillin. Following dilution into fresh media, cultures were grown for 5 hr shaking at 37°C. To study *phoN::TnphoA* reporter activation in the presence of CAMP, overnight cultures were washed once in N-minimal media pH 7.5 containing 1 mM MgCl₂ and diluted 1:100 into the same growth media. Cultures were then grown to OD₆₀₀ 0.2, treated with 5 μg•ml⁻¹ of C18G peptide (Anaspec, Fremont, CA), and grown shaking at 37°C for 90 min. Following incubation, alkaline phosphatase activity was measured. Alkaline phosphatase activity assays were performed according to standard protocol on cultures grown in duplicate and repeated on at least three independent occasions.

Genetic techniques

All PhoQ alleles with point-mutations were generated on pBAD24-*phoQ* or pET11a-*phoQ* using the appropriate primers pairs (**Table 3**) and a standard site-directed mutagenesis protocol or Gibson assembly (Gibson et al., 2009). To generate *phoQ*^{W104C-A128C} on the *S. enterica* Typhimurium 14028s chromosome, lambda red allelic exchange methods were utilized (Gerlach et al., 2007). Briefly, to engineer *phoQ*^{W104C-A128C} on the *S. enterica* Typhimurium chromosome, a tetracycline resistant cassette (*tetRA*) was amplified using primers KH45 and KH46. The resulting *phoQ::tetRA* amplicon was recombined into CS093 generating *phoQ::tetRA* (KH23). Primers KH93 and KH94 were used to amplify *phoQ*^{W104C-A128C} from pBAD24-*phoQ*^{W104C-A128C} (CS1382). The *phoQ*^{W104C-A128C} amplicon was

Table 2. Strains and plasmids used in this study

Strain	Description	Source
CS093	14028s wild type <i>S. enterica</i> Typhimurium	ATCC
CS1081	CS093 <i>phoQ::TPOP phoN::TnpA</i>	Bader et al., 2005
CS1083	CS1081 pBAD24	Bader et al., 2005
CS1084	CS1081 pBAD24- <i>phoQ</i>	Bader et al., 2005
CS1399	CS1081 pBAD24- <i>phoQ</i> ^{I88N}	This work
CS1400	CS1081 pBAD24- <i>phoQ</i> ^{Y89N}	This work
KH45	CS1081 pBAD24- <i>phoQ</i> ^{I102C}	This work
KH140	CS1081 pBAD24- <i>phoQ</i> ^{L105D}	This work
CS1402	CS1081 pBAD24- <i>phoQ</i> ^{T124N}	This work
CS1403	CS1081 pBAD24- <i>phoQ</i> ^{V126E}	This work
CS1404	CS1081 pBAD24- <i>phoQ</i> ^{T129I}	This work
CS1405	CS1081 pBAD24- <i>phoQ</i> ^{T131P}	This work
CS1406	CS1081 pBAD24- <i>phoQ</i> ^{L132P}	This work
KH28	CS1081 pBAD24- <i>phoQ</i> ^{L133C}	This work
CS1407	CS1081 pBAD24- <i>phoQ</i> ^{D150G}	This work
CS1408	CS1081 pBAD24- <i>phoQ</i> ^{A153P}	This work
CS1409	CS1081 pBAD24- <i>phoQ</i> ^{M155V}	This work
CS1410	CS1081 pBAD24- <i>phoQ</i> ^{V178D}	This work
CS1374	CS1081 pBAD24- <i>phoQ</i> ^{W104C}	This work
CS1386	CS1081 pBAD24- <i>phoQ</i> ^{A128C}	This work
CS1382	CS1081 pBAD24- <i>phoQ</i> ^{W104C-A128C}	This work
KH48	CS1081 pBAD24- <i>phoQ</i> ^{W104S}	This work
KH49	CS1081 pBAD24- <i>phoQ</i> ^{A128S}	This work
KH50	CS1081 pBAD24- <i>phoQ</i> ^{W104S A128S}	This work
CS1101	BL21 pET11a- <i>phoQ</i> 45-190-(His) ₆	Bader et al., 2005
KH85	NEB SHuffle T7 express pET11a- <i>phoQ</i> ^{W104C-A128C} 45-190-(His) ₆	This work
KH23	<i>phoQ::tetRA</i>	This work
KH163	<i>phoQ</i> ^{W104C-A128C}	This work
CS1350	Δ <i>phoQ</i>	Prost et al., 2008
KH127	<i>phoQ phoN105::TnpA</i>	This work
KH130	<i>phoQ</i> ^{W104C-A128C} <i>phoN105::TnpA</i>	This work
KH111	CS093 pWSK129 ^{Kan}	This work
KH112	CS093 pWSK29 ^{Amp}	This work
KH113	<i>phoQ</i> ^{W104C-A129C} pWSK29 ^{Amp}	This work
KH114	Δ <i>phoQ</i> pWSK29 ^{Amp}	This work

DOI: [10.7554/eLife.06792.016](https://doi.org/10.7554/eLife.06792.016)

recombined into *phoQ::tetRA* (KH23). Positive clones for *phoQ*^{W104C-A128C} recombination were identified via Bochner selection (**Bochner et al., 1980**). Chromosomal *phoQ*^{W104C-A128C} was then transduced into a clean *S. enterica* Typhimurium 14028s background via P22 phage transduction. *phoQ*^{W104C-A128C} positive clones were confirmed via DNA sequencing.

To identify residues in the PhoQ PD that when mutated result in increased *phoN::TnpA* activity, we performed a random mutagenesis screen as previously described (**Cho et al., 2006**). Briefly, pBAD24-*phoQ* was randomly mutagenized using primers LP135 and LP136 to introduce one mutation per 500 bp in the *phoQ* PD using the GeneMorph II EZClone Domain Mutagenesis Kit

Table 3. Primer sequences used in this study

Primer # (name)	Sequence (5'–3')
LP135 (RM_Fwd)	CTGGTCGGCTATAGCGTAAGTTTTG
LP136 (RM_Rev)	CACGTATACGAACCAGCTCCACAC
LP178 (I88N_Fwd)	CGACCATGACGCTGAATTACGATGAAACGG
LP179 (I88N_Rev)	CCGTTTCATCGTAATTCAGCGTCATGGTCG
LP180 (Y89N_Fwd)	CCATGACGCTGATTAACGATGAAACGGGC
LP181 (Y89N_Rev)	GCCC GTTTCATCGTTAATCAGCGTCATGG
KH81 (I102C_Fwd)	GACGCAGCGCAACTGTCCTGGCTGATTAAG
KH82 (I102C_Rev)	CTTTTAATCAGCCAGGGACAGTTGCGCTGCGTC
LP184 (T124N_Fwd)	CTTCCATGAAATTGAAAACAACGTAGACGCCACC
LP185 (T124N_Rev)	GGTGGCGTCTACGTTGTTTTCAATTCATGGAAG
LP186 (V126E_Fwd)	GAAATTGAAACCAACGAAGACGCCACCAGCAC
LP187 (V126E_Rev)	GTGCTGGTGGCGTCTTCGTTGGTTTCAATTC
LP188 (T129I_Fwd)	CAACGTAGACGCCATCAGCAGCGCTGTTG
LP189 (T129I_Rev)	CAACAGCGTGCTGATGGCGTCTACGTTG
KH192 (L105D_Fwd)	GCGCAACATTCCTGGGATATTAAGCATTCAAC
KH193 (L105D_Rev)	GTTGAATGCTTTAATATCCCAGGGAATGTTGCGC
LP190 (L131P_Fwd)	CAACGTAGACGCCACCAGCCACTGTTGAGCGAAGACCATTG
LP191 (L131P_Rev)	GAATGGTCTTCGCTCAACAGTGGGCTGGTGGCGTCTACGTTG
LP192 (L132P_Fwd)	GACGCCACCAGCAGCCATTGAGCGAAGACCATTG
LP193 (L132P_Rev)	GAATGGTCTTCGCTCAATGGCGTGCTGGTGGCGTC
KH85 (L133C_Fwd)	CACCAGCAGCTGTGTAGCGAAGACCATTG
KH86 (L133C_Rev)	GAATGGTCTTCGCTACACAGCGTGCTGGTG
LP194 (D150G_Fwd)	GTACGTGAAGATGGCGATGATGCCGAG
LP195 (D150G_Rev)	CTCGGCATCATCGCCATCTTCACGTAC
LP196 (A153P_Fwd)	GAAGATGACGATGATCCCGAGATGACCCAC
LP197 (A153_Rev)	GTGGGTCATCTCGGGATCATCGTCATCTTC
LP198 (M155V_Fwd)	GACGATGATGCCGAGGTAACCCACTCGGTAGC
LP199 (M155V_Rev)	GCTACCGAGTGGGTTACCTCGGCATCATCGTC
LP200 (V178D_Fwd)	CCATCGTGGTGGACGATACCATTCCG
LP201 (V178D_Rev)	CGGAATGGTATCGTCCACCACGATGG
LP141 (W104C_Fwd)	GCGCAACATTCCTGCCTGATTAAGCATTG
LP142 (W104C_Rev)	GAATGCTTTAATCAGGCAGGGAATGTTGCGC
LP145 (A128C_Fwd)	GAAACCAACGTAGACTGCACCAGCAGCTGTTG
LP146 (A128C_Rev)	CAACAGCGTGCTGGTGCAGTCTACGTTGGTTTC
KH61 (W104S_Fwd)	CAGCGCAACATTCAGCCTGATTAAGCATTG
KH62 (W104S_Rev)	GAATGCTTTAATCAGGCTGGGAATGTTGCGCTG
KH63 (A128S_Fwd)	GAAACCAACGTAGACAGCACCAGCAGCTGTTG
KH64 (A128S_Rev)	CAACAGCGTGCTGGTGTCTACGTTGGTTTC
LP164 (T48C_Fwd)	GTAAGTTTTGATAAACCTGCTTCGTTGCTGCGCG
LP165 (T48C_Rev)	CGCGCAGCAAACGAAAGCAGGTTTTATCAAACCTTAC
LP168 (K186C_Fwd)	CCATTCCGATAGAATATGCCGCTCTATATGGTGTG
LP169 (K186C_Rev)	CACACCATATAGGAGCGGCATAGTTCTATCGGAATGG
KH35 (T48S_Fwd)	GTTTTGATAAACCTGCTTCGTTGCTGCGCG
KH36 (T48S_Rev)	CGCAGCAAACGAAAGCTGTTTTATCAAAA

Table 3. Continued on next page

Table 3. Continued

Primer # (name)	Sequence (5'–3')
KH39 (K186S_Fwd)	CATTCCGATAGAACTAAGTCGCTCCTATATGGTG
KH40 (K186S_Rev)	CACCATATAGGAGCGACTTAGTTCTATCGGAATG
KH45 (PhoQ_tetRA_knock-in_Fwd)	GAATAAATTTGCTCGCCATTTTCTGCCGCTGTCGCTGCGGTTAAGACCCA CTTTCACA
KH46 (PhoQ_tetRA_knock-in_Rev)	CCTCTTTCTGTGTGGGATGCTGTGGCCAAAAACGACCTCCTAAGCACTT GTCTCCTG
KH93 (ST-PhoQ_N-term_Fwd)	ATGAATAAATTTGCTCGCCATTTTC
KH94 (ST-PhoQ_N-term_Rev)	TTATTCCTCTTTCTGTGTGGG
KH265 (ST-rpoD_Fwd_qRT)	GGGATCAACCAGGTTCAATG
KH266 (ST-rpoD_Rev_qRT)	GGACAAAACGAGCCTCTTCAG
KH269 (ST-pagD_Fwd_qRT)	G TTCAGGCCATTGTTCTGGT
KH270 (ST-pagD_Rev_qRT)	TAATCTGCCTGGCTTGCTTT
KH273 (ST-pagO_Fwd_qRT)	CGGGCTTAACTATCGCAATC
KH274 (ST-pagO_Rev_qRT)	CAGCAGAAATAAGCGCAGTG
KH275 (ST-phoP_Fwd_qRT)	TGCCAGGGAAGCTGATTACT
KH276 (ST-phoP_Rev_qRT)	CAGCGGCGTATTAAGGAAA
KH277 (ST-phoN_Fwd_qRT)	CCGGCTTACCGCTATGATAA
KH278 (ST-phoN_Rev_qRT)	CGTTACATCTGCATCCTCA

DOI: [10.7554/eLife.06792.017](https://doi.org/10.7554/eLife.06792.017)

(Agilent Technologies, Santa Clara, CA). The resulting mutagenized pBAD24-*phoQ* plasmids were transformed into CS1081 and grown overnight on LB plates containing XP substrate (Sigma 104, Sigma-Aldrich Corp., St. Louis, MO), ampicillin $100 \mu\text{g}\cdot\text{ml}^{-1}$, and 10 mM MgCl_2 . In the morning, plates were screened for blue colonies indicative of *phoN::TnpA* alkaline phosphatase activity and PhoQ activation by divalent cation limitation. Approximately, 50,000 colonies were screened. 103 blue colonies were chosen and sequenced, yielding 26 single amino acid substitutions. Mutations identified in the screen were independently engineered in a clean pBAD24-*phoQ* background using the appropriate primers pairs (Table 3) and a standard site-directed mutagenesis protocol. Phenotypes were confirmed by alkaline phosphatase activity assays in duplicate on at least three separate occasions.

Protein expression and purification

The PhoQ PD (strain CS1101) was purified as previously described (Bader et al., 2005). PhoQ^{W104C-A128C} PD (strain KH85) was purified from SHuffle T7 Express *E. coli* (NEB, Ipswich, MA). Purification and storage of PhoQ^{W104C-A128C} PD was performed according to the same methods as wild-type PhoQ PD. Disulfide bond formation in PhoQ^{W104C-A128C} PD was confirmed by SDS-PAGE. Briefly, strain CS1101 or KH85 were grown in LB media supplemented with $100 \text{ mg}\cdot\text{l}^{-1}$ ampicillin for all non-labeling experiments. For ¹⁵N-labeling and NMR experiments, strain CS1101 was grown in MOPS minimal medium supplemented with $100 \text{ mg}\cdot\text{l}^{-1}$ ampicillin and $1 \text{ g}\cdot\text{l}^{-1}$ ¹⁵N-ammonium chloride. Expression strains were grown to mid-log phase and IPTG was added to 0.5 mM . Cultures were induced for 4–6 hr, harvested by centrifugation and lysed using a French Pressure Cell. Inclusion bodies were isolated by centrifugation, washed once in 50 mM sodium phosphate pH 8.0 300 mM NaCl , resuspended in 20 mM sodium phosphate pH 8.0 100 mM NaCl 7 M urea , and incubated on ice for 1 hr. Samples were then ultracentrifuged at $50,000 \text{ rpm}$ for 30 min. The supernatant was rapidly diluted into ice cold 20 mM sodium phosphate pH 8.0. Samples were filtered and purified using a 5 ml HisTrap HP nickel column (GE Healthcare Bio-Sciences, Pittsburgh, PA) according to standard protocol. Purified protein was then applied to a Superdex-200 gel filtration column (GE Healthcare Bio-Sciences) equilibrated with 20 mM sodium phosphate pH 6.5 150 mM NaCl 0.1 mM EDTA . PhoQ containing fractions were pooled, concentrated to approximately 0.25 mM and stored at -80°C in 10% glycerol. PhoQ^{W104C-A128C} PD was expressed by growing strain KH85 at 37°C to mid log phase in LB medium supplemented with $100 \text{ mg}\cdot\text{l}^{-1}$ ampicillin. IPTG was added to 0.5 mM and protein expression was maintained overnight at 20°C .

NMR spectroscopy and analysis

(¹H, ¹⁵N)-HSQC-NMR spectra of PhoQ PD were collected as a function of pH previously (Prost et al., 2007). Briefly, uniformly ¹⁵N- and ¹³C-labeled PhoQ PD was prepared to 1.2 mM in 20 mM sodium phosphate buffer pH 6.5, 150 mM NaCl, 20 mM MgCl₂, 0.1 mM EDTA, and 10% (vol/vol) D₂O. The pH was lowered by approximately 0.5 units at a time by addition of microliter aliquots of 500 mM DCl. HSQC spectra from the pH-titration were collected at pH 6.5, 6.0, 5.5, 4.9, 4.1, and 3.5. Standard triple-resonance experiments were collected a pH 3.5 for assignments. Assignments from pH 3.5 were translated to higher pH conditions by tracking chemical shifts through the titration series. NMR experiments were performed at 25°C on a Bruker DMX 500 MHz spectrometer equipped with a triple-resonance, triple-axis gradient probe. Data were processed and analyzed using the programs NMRPipe/NMRDraw (Delaglio et al., 1995) and NMRView (Johnson and Blevins, 1994).

To identify regions of the PhoQ PD affected by pH, (¹H, ¹⁵N)-HSQC-NMR spectra of the PhoQ PD were compared at pH 6.5 and 3.5. Resonances that experienced a chemical shift perturbation (CSP) greater than 0.08 ppm and/or that broadened beyond detection were considered significantly affected by pH. CSPs were calculated using the formula $(\Delta^1\text{H}) + (\Delta^{15}\text{N}/5)^{1/2}$. Resonances that did not meet these criteria were considered unaffected. 36 residues within the PhoQ PD could not be unambiguously categorized into these groups because of missing/ambiguous assignments and/or crowding in the spectra.

Bacterial gene expression from growth in N-minimal media

Wild-type (CS093), *phoQ*^{W104C-A128C} (KH163), and Δ *phoQ* (CS1350) *S. enterica* Typhimurium were grown overnight in N-mm 1 mM MgCl₂ pH 7.5. In the morning, the cultures were normalized to OD₆₀₀ 2.0 and diluted 1:50 into fresh N-mm 1 mM MgCl₂ pH 7.5 and grown at 37°C, 250 rpm. At approximately OD₆₀₀ 0.2, the cultures were normalized to OD₆₀₀ 0.2•ml⁻¹, washed once, and resuspended in 1 ml of either N-mm pH 7.5 1 mM MgCl₂, pH 5.5 1 mM MgCl₂, pH 7.5 10 μM MgCl₂, or pH 7.5 1 mM MgCl₂ 5 μg•ml⁻¹. The cultures were grown shaking at 37°C, 250 rpm. After 1 hr, the cultures were immediately pelleted at 4°C, the media was aspirated, and placed on ice. RNA was collected using the Trizol Max Bacterial RNA Isolation Kit (Ambion, Thermo Fisher Scientific, Grand Island, NY) and RNeasy mini kit (Qiagen, Netherlands). cDNA was generated using SuperScript III First-Strand (Invitrogen, Thermo Fisher Scientific, Grand Island, NY).

Synthesis Supermix for qRT-PCR (Invitrogen). Quantitative RT-PCR was performed using SYBR GreenER qPCR SuperMix Universal (Invitrogen) and a BioRad CFX96 thermocycler for *S. enterica* Typhimurium *rpoD*, *pagD*, *pagO*, *phoN*, and *phoP* target transcripts using the appropriate qRT primers (Table 3). Relative gene expression was determined using the 2^{-ΔΔC_T} method (Livak and Schmittgen, 2001). *rpoD* was used as the calibrator and gene expression was normalized to Δ *phoQ*.

Protein crystallization, data collection, and structure determination

The *S. enterica* Typhimurium PhoQ^{W104C-A128C} PD structure (PDB 4UEY) was acquired by crystallizing the purified protein using a Mosquito crystallization robot (TTP Labtech, United Kingdom) and Nextal Classic Suite, Nextal Classic Suite II, Protein complex Suite (Qiagen) and JBScreen Classic HTS II (Jena Bioscience, Germany). The progress of crystallization at 20°C was monitored using a temperature controlled robot (Rock imager system, Formulatrix, Bedford, MA). Crystals appeared after 2 weeks. Optimized crystals of the PhoQ^{W104C-A128C} PD were formed in 0.1 M Bis-Tris pH 6.5 200 mM Magnesium chloride 25% (wt/vol) PEG3350. Crystals of the PhoQ^{W104C-A128C} PD were mounted in nylon loops (Hampton Research, Aliso Viejo, CA) and directly frozen in liquid nitrogen. Diffraction data of the crystals were collected at ALBA synchrotron (BL13 XALOC, Barcelona, Spain). Crystals were kept at 100 K and 200 diffraction images at 1° were recorded on a Pilatus 6M detector (Dectris, Baden, Switzerland). Diffraction data were processed and scaled using the XDS software package (Kabsch, 2010). Data were truncated at lower resolution according to the recently defined CC* correlation factor (Karplus and Diederichs, 2012). Molecular replacement trials were performed using the program MOLREP and the model of the *S. enterica* Typhimurium PhoQ PD from the PDB databank (PDB 1YAX) (Cho et al., 2006; Vagin and Teplyakov, 2010). The structure was refined using the PHENIX program package (Afonine et al., 2012) after rebuilding the structure in COOT (Emsley et al., 2010). Structure details and PDB entries are given in Table 1. Model quality was assessed using the Molprobity server (<http://molprobity.biochem.duke.edu/>).

Circular dichroism

Prior to CD data collection, purified PhoQ PD and PhoQ^{W104C-A128C} PD were exchanged into 20 mM sodium phosphate buffer pH 5.5 150 mM NaCl 1 mM MgCl₂ using a 5 ml HiTrap desalting column (Amersham) and treated with or without an approximate 1000 molar excesses of TCEP hydrochloride (Sigma) pH 5.5 for 4 hr to reduce the disulfide bond formed between W104C and A128C. Following TCEP treatment, protein samples were exchanged in to 20 mM sodium phosphate buffer pH 5.5 150 mM NaCl 1 mM MgCl₂, with or without 1 mM TCEP and equilibrated overnight at 4°C. Following buffer exchange and equilibration, protein samples were concentrated and prepared to 17 μM for CD analysis. Disulfide bond reduction was monitored by SDS-PAGE prior to performing CD experiments. All CD data collection was performed on an Aviv model 420 spectrometer fitted with a total fluorescence accessory module and thermoelectric cuvette holder using a 1 mm pathlength quartz cuvette. Wavelength scans were performed for each sample prior to thermal denaturation from 260 to 195 nm at 25°C, sampling every 1 nm, with a 3 s averaging time per reading. CD-monitored thermal denaturation data was collected at 212 nm, from 25°C to 95°C, in 1°C increments, with a 3 s averaging time per reading, and 30 s temperature equilibration between readings. Raw thermal denaturation data were normalized to give the fraction unfolded protein assuming a two-state denaturation process (Kamal et al., 2002). All CD experiments were reproduced on at least three separate occasions.

Mouse infections

BALB/c or A/J mice were ordered from Jackson Laboratories and virulence phenotypes for strains of *S. enterica* Typhimurium were determined by competition or single-strain inoculation. Competition experiments were performed similarly to previously described (Freeman et al., 2003). Briefly, cultures of KH111, KH112, KH113, and KH114 were grown overnight in LB media with the appropriate antibiotic and prepared by serial dilution in PBS. The inoculum for IP competition experiments was prepared by equally mixing 2.5×10^5 cfu of KH111 (strain A) with 2.5×10^5 cfu of KH112, KH113, or KH114 (strain B) in 2 ml PBS. The inoculum for PO competition experiments was prepared by equally mixing 5×10^7 cfu of KH111 (strain A) with 5×10^7 cfu of KH112, KH113, or KH114 (strain B) in 2 ml PBS. 6- to 8-week old female BALB/c mice were administered 0.2 ml of the mixture, for a total inoculation of 1×10^5 bacteria for IP infections or 5×10^8 bacteria for PO infections. For PO competition experiments, mice were deprived food for 5 hr prior to administering bacteria by oral gavage. The inoculum was confirmed for each experiment by plating dilutions on LB media supplemented with either $50 \mu\text{g}\cdot\text{ml}^{-1}$ kanamycin or $100 \mu\text{g}\cdot\text{ml}^{-1}$ ampicillin. Mice were euthanized by CO₂ asphyxiation at 48-hpi (IP) or 96-hpi (PO) and spleens were harvested and homogenized in PBS. Homogenized spleens were serially diluted and plated on LB media supplemented with either $50 \mu\text{g}\cdot\text{ml}^{-1}$ kanamycin or $100 \mu\text{g}\cdot\text{ml}^{-1}$ ampicillin in order to determine the $\text{cfu}\cdot\text{ml}^{-1}$ bacterial burden for each strain. The competitive index (CI) for each strain was calculated using the following formula: $\text{CI} = (\text{strain B } \text{cfu}\cdot\text{ml}^{-1} \text{ spleen} / \text{strain A } \text{cfu}\cdot\text{ml}^{-1} \text{ spleen}) / (\text{strain B } \text{cfu}\cdot\text{ml}^{-1} \text{ inoculum} / \text{strain A } \text{cfu}\cdot\text{ml}^{-1} \text{ inoculum})$.

For single-strain experiments, cultures of CS093, KH163, and CS1350 were grown overnight in LB media and prepared by serial dilution in PBS. The inoculum was confirmed for each experiment by plating dilutions on LB media. 6- to 8-week old female BALB/c or A/J mice were infected IP with approximately 1×10^3 cfu in 0.2 ml PBS. Mice were euthanized by CO₂ asphyxiation at 48- and 96-hpi and spleens were harvested and homogenized in PBS. Homogenized spleens were serially diluted and plated on LB media in order to determine the $\text{cfu}\cdot\text{ml}^{-1}$ bacterial burden for each strain. All mouse experiments were performed with IACUC approval.

Bacterial growth curve

Wild type (CS093), *phoQ*^{W104C-A128C} (KH163), and ΔphoQ (CS1350) were grown overnight in N-mm pH 7.5 1 mM MgCl₂. The following morning, the strains were washed in the appropriate N-mm, normalized, and diluted to 0.05 OD₆₀₀ in either N-mm pH 7.5 or pH 5.5 supplemented with 1 mM MgCl₂. The strains were grown in a rolling drum at 37°C. At the indicated time-points, the bacterial strains were diluted 1:10 in PBS and their OD₆₀₀ was monitored.

Macrophage growth conditions and infections

Bone marrow was isolated from the femurs of BALB/c mice obtained from Jackson Laboratories and differentiated for 7 days in RPMI 1640 media (Gibco #22400-089, Thermo Fisher Scientific, Grand

Island, NY) supplemented with 10% FBS and L-929 cell supernatant following standard protocols. Following differentiation, bone-marrow derived macrophages were seeded into 24-well plates and incubated overnight. Bone-marrow derived macrophages were infected in triplicate with CS093, KH163, or CS1350 *S. enterica* Typhimurium and bacterial survival determined using a standard gentamicin-protection assay. Briefly, CS093, KH163, and CS1350 were grown overnight in LB media. The following morning, bacterial cultures are washed in PBS and suspended in RPMI 1640 at the appropriate concentration. BALB/c bone-marrow derived macrophages in 24-well plates (2×10^5 per well) were washed with PBS and infected in triplicate with CS093, KH163, or CS1350 (M.O.I. of 10) in RPMI 160 supplemented with 10% FBS, synchronized by centrifugation at 1000 rpm for 5 min at RT, and incubated for 30 min. Following incubation, infected macrophage monolayers were washed with PBS, incubated with media supplemented with $100 \mu\text{g}\cdot\text{ml}^{-1}$ gentamicin⁻¹ (Sigma) for 90 min and maintained at $15 \mu\text{g}\cdot\text{ml}^{-1}$ gentamicin for the duration of the experiment. Bacterial intracellular survival was determined by lysing infected macrophage with 1% Triton X-100 in PBS at the indicated time-points and plating serial dilutions on LB media for cfu counting.

Bacterial gene expression from within infected macrophage

BALB/c bone marrow-derived macrophages were seeded into 6-well plates (1×10^7 per well) and infected in triplicate with CS093, KH163, or CS1350 *S. enterica* Typhimurium using a standard gentamicin-protection protocol. 30 min post-infection, extracellular bacteria were harvested, lysed in Max Bacterial Enhancement Reagent (Ambion) and RNA was stabilized with Trizol (Ambion). 4 hr post-infection, media was aspirated, infected macrophages were solubilized in Trizol to stabilize total RNA and triplicates were pooled. Trizol samples were stored at -80°C . RNA was prepared according to the Trizol Reagent protocol, treated with TURBO DNA-free DNase (Ambion), and RNA quality was monitored using a 2200 TapeStation (Agilent Technologies). cDNA was generated using SuperScript III First-Strand Synthesis Supermix for qRT-PCR (Invitrogen). Quantitative RT-PCR was performed using SYBR GreenER qPCR SuperMix Universal (Invitrogen) and a BioRad CFX96 thermocycler for *S. enterica* Typhimurium *rpoD*, *pagD*, *pagO*, *phoN*, and *phoP* target transcripts using the appropriate qRT primers (Table 3). Relative gene expression was determined using the $2^{-\Delta\Delta C_T}$ method (Livak and Schmittgen, 2001). *rpoD* cDNA generated from extracellular bacteria harvested 30 min post-infection was used as the calibrator.

Three-dimensional structural analysis

Analysis and modeling of the three-dimensional protein structures was carried out using the PyMOL molecular viewer (Schrodinger, 2010).

Acknowledgements

We would like to thank C Davey, Z Dalebroux, H Kulasekara, A Imhaus, J Fan, and S Matamouros for constructive feedback, A Hajjar for assistance with mouse infections, D Baker and F Parmeggiani for CD spectrometer assistance, and A Rojas at ALBA synchrotron for data collection. This work was funded by grant R01AI030479 from the NIAID to S.I.M.

Additional information

Funding

Funder	Grant reference	Author
National Institute of Allergy and Infectious Diseases (NIAID)	R01AI030479	Samuel I Miller

The funder had no role in study design, data collection and interpretation, or the decision to submit the work for publication.

Author contributions

KGH, Conception and design, Acquisition of data, Analysis and interpretation of data, Drafting or revising the article, Contributed unpublished essential data or reagents; SPD, Conception and design, Acquisition of data, Analysis and interpretation of data, Drafting or revising the article; ES-V,

KZ, Acquisition of data, Analysis and interpretation of data, Drafting or revising the article; M-PB, LRP, MED, Conception and design, Acquisition of data, Analysis and interpretation of data; KKD, Acquisition of data, Analysis and interpretation of data, Drafting or revising the article, Contributed unpublished essential data or reagents; REK, SIM, Conception and design, Analysis and interpretation of data, Drafting or revising the article

Ethics

Animal experimentation: This study was performed in strict accordance with the recommendations in the Guide for the Care and Use of Laboratory Animals of the National Institutes of Health. All of the animals were handled according to approved institutional animal care and use committee (IACUC) protocol (2982-02) of the University of Washington.

Additional files

Major datasets

The following dataset was generated:

Author(s)	Year	Dataset title	Dataset ID and/or URL	Database, license, and accessibility information
Sancho-Vaello E, Hicks KG, Miller SI, Zeth K	2015	Structure of the periplasmic domain PhoQ double mutant (W104C-A128C)	http://www.rcsb.org/pdb/search/structidSearch.do?structureId=4UEY	Publicly available at RCSB Protein Data Bank (Accession no: 4UEY).

The following previously published datasets were used:

Author(s)	Year	Dataset title	Dataset ID and/or URL	Database, license, and accessibility information
Cho US, Bader MW, Amaya MF, Daley ME, Klevit RE, Miller SI, Xu W	2006	Crystal structure Analysis of <i>S. typhimurium</i> PhoQ sensor domain with Calcium	http://www.rcsb.org/pdb/explore/explore.do?structureId=1YAX	Publicly available at RCSB Protein Data Bank (Accession no: 1YAX).
Cheung J, Bingman CA, Reyngold M, Hendrickson WA, Waldburger CD	2008	Crystal Structure of the <i>E. coli</i> PhoQ Sensor Domain	http://www.rcsb.org/pdb/explore/explore.do?structureId=3BQ8	Publicly available at RCSB Protein Data Bank (Accession no: 3BQ8).

References

- Adams P, Fowler R, Kinsella N, Howell G, Farris M, Coote P, O'Connor CD. 2001. Proteomic detection of PhoPQ- and acid-mediated repression of *Salmonella* motility. *Proteomics* 1:597–607. doi: [10.1002/1615-9861\(200104\)1:4<597::AID-PROT597>3.0.CO;2-P](https://doi.org/10.1002/1615-9861(200104)1:4<597::AID-PROT597>3.0.CO;2-P).
- Afonine PV, Grosse-Kunstleve RW, Echols N, Headd JJ, Moriarty NW, Mustyakimov M, Terwilliger TC, Urzhumtsev A, Zwart PH, Adams PD. 2012. Towards automated crystallographic structure refinement with phenix.refine. *Acta Crystallographica Section D, Biological Crystallography* 68:352–367. doi: [10.1107/S0907444912001308](https://doi.org/10.1107/S0907444912001308).
- Alpuche Aranda CM, Swanson JA, Loomis WP, Miller SI. 1992. *Salmonella typhimurium* activates virulence gene transcription within acidified macrophage phagosomes. *Proceedings of the National Academy of Sciences of USA* 89:10079–10083. doi: [10.1073/pnas.89.21.10079](https://doi.org/10.1073/pnas.89.21.10079).
- Bader MW, Navarre WW, Shiao W, Nikaido H, Frye JG, McClelland M, Fang FC, Miller SI. 2003. Regulation of *Salmonella typhimurium* virulence gene expression by cationic antimicrobial peptides. *Molecular Microbiology* 50:219–230. doi: [10.1046/j.1365-2958.2003.03675.x](https://doi.org/10.1046/j.1365-2958.2003.03675.x).
- Bader MW, Sanowar S, Daley ME, Schneider AR, Cho U, Xu W, Klevit RE, Le Moual H, Miller SI. 2005. Recognition of antimicrobial peptides by a bacterial sensor kinase. *Cell* 122:461–472. doi: [10.1016/j.cell.2005.05.030](https://doi.org/10.1016/j.cell.2005.05.030).
- Bearson BL, Wilson L, Foster JW. 1998. A low pH-inducible, PhoPQ-dependent acid tolerance response protects *Salmonella typhimurium* against inorganic acid stress. *Journal of Bacteriology* 180:2409–2417.
- Behlau I, Miller SI. 1993. A PhoP-repressed gene promotes *Salmonella typhimurium* invasion of epithelial cells. *Journal of Bacteriology* 175:4475–4484.
- Belden WJ, Miller SI. 1994. Further characterization of the PhoP regulon: identification of new PhoP-activated virulence loci. *Infection and Immunity* 62:5095–5101.
- Bochner BR, Huang HC, Schieven GL, Ames BN. 1980. Positive selection for loss of tetracycline resistance. *Journal of Bacteriology* 143:926–933.
- Cano DA, Martinez-Moya M, Pucciarelli MG, Groisman EA, Casadesús J, Garcia-Del Portillo F. 2001. *Salmonella enterica* serovar Typhimurium response involved in attenuation of pathogen intracellular proliferation. *Infection and Immunity* 69:6463–6474. doi: [10.1128/IAI.69.10.6463-6474.2001](https://doi.org/10.1128/IAI.69.10.6463-6474.2001).

- Casey JR, Grinstein S, Orlowski J. 2010. Sensors and regulators of intracellular pH. *Nature Reviews. Molecular Cell Biology* **11**:50–61. doi: [10.1038/nrm2820](https://doi.org/10.1038/nrm2820).
- Castelli ME, Garcia Véscovi E, Soncini FC. 2000. The phosphatase activity is the target for Mg²⁺ regulation of the sensor protein PhoQ in *Salmonella*. *The Journal of Biological Chemistry* **275**:22948–22954. doi: [10.1074/jbc.M909335199](https://doi.org/10.1074/jbc.M909335199).
- Chen HD, Groisman EA. 2013. The biology of the PmrA/PmrB two-component system: the major regulator of lipopolysaccharide modifications. *Annual Review of Microbiology* **67**:83–112. doi: [10.1146/annurev-micro-092412-155751](https://doi.org/10.1146/annurev-micro-092412-155751).
- Cheung J, Bingman CA, Reyngold M, Hendrickson WA, Waldburger CD. 2008. Crystal structure of a functional dimer of the PhoQ sensor domain. *The Journal of Biological Chemistry* **283**:13762–13770. doi: [10.1074/jbc.M710592200](https://doi.org/10.1074/jbc.M710592200).
- Cheung J, Hendrickson WA. 2008. Crystal structures of C4-dicarboxylate ligand complexes with sensor domains of histidine kinases DcuS and DctB. *The Journal of Biological Chemistry* **283**:30256–30265. doi: [10.1074/jbc.M805253200](https://doi.org/10.1074/jbc.M805253200).
- Cheung J, Hendrickson WA. 2010. Sensor domains of two-component regulatory systems. *Current Opinion in Microbiology* **13**:116–123. doi: [10.1016/j.mib.2010.01.016](https://doi.org/10.1016/j.mib.2010.01.016).
- Cho US, Bader MW, Amaya MF, Daley ME, Klevit RE, Miller SI, Xu W. 2006. Metal bridges between the PhoQ sensor domain and the membrane regulate transmembrane signaling. *Journal of Molecular Biology* **356**:1193–1206. doi: [10.1016/j.jmb.2005.12.032](https://doi.org/10.1016/j.jmb.2005.12.032).
- Choi CH, Webb BA, Chimenti MS, Jacobson MP, Barber DL. 2013. pH sensing by FAK-His58 regulates focal adhesion remodeling. *The Journal of Cell Biology* **202**:849–859. doi: [10.1083/jcb.201302131](https://doi.org/10.1083/jcb.201302131).
- Christensen KA, Myers JT, Swanson JA. 2002. pH-dependent regulation of lysosomal calcium in macrophages. *Journal of Cell Science* **115**:599–607.
- Dalebroux ZD, Matamouros S, Whittington D, Bishop RE, Miller SI. 2014. PhoPQ regulates acidic glycerophospholipid content of the *Salmonella* Typhimurium outer membrane. *Proceedings of the National Academy of Sciences of USA* **111**:1963–1968. doi: [10.1073/pnas.1316901111](https://doi.org/10.1073/pnas.1316901111).
- Dalebroux ZD, Miller SI. 2014. Salmonellae PhoPQ regulation of the outer membrane to resist innate immunity. *Current Opinion in Microbiology* **17**:106–113. doi: [10.1016/j.mib.2013.12.005](https://doi.org/10.1016/j.mib.2013.12.005).
- Dawson JE, Seckute J, De S, Schueler SA, Oswald AB, Nicholson LK. 2009. Elucidation of a pH-folding switch in the *Pseudomonas syringae* effector protein AvrPto. *Proceedings of the National Academy of Sciences of USA* **106**:8543–8548. doi: [10.1073/pnas.0809138106](https://doi.org/10.1073/pnas.0809138106).
- Dean RT, Jessup W, Roberts CR. 1984. Effects of exogenous amines on mammalian cells, with particular reference to membrane flow. *The Biochemical Journal* **217**:27–40.
- Delaglio F, Grzesiek S, Vuister GW, Zhu G, Pfeifer J, Bax A. 1995. NMRPipe: a multidimensional spectral processing system based on UNIX pipes. *Journal of Biomolecular NMR* **6**:277–293. doi: [10.1007/BF00197809](https://doi.org/10.1007/BF00197809).
- Ellermeier CD, Slauch JM. 2004. RtsA coordinately regulates DsbA and the *Salmonella* pathogenicity island 1 type III secretion system. *Journal of Bacteriology* **186**:68–79. doi: [10.1128/JB.186.1.68-79.2004](https://doi.org/10.1128/JB.186.1.68-79.2004).
- Emsley P, Lohkamp B, Scott WG, Cowtan K. 2010. Features and development of coot. *Acta Crystallographica Section D, Biological Crystallography* **66**:486–501. doi: [10.1107/S0907444910007493](https://doi.org/10.1107/S0907444910007493).
- Fields PI, Groisman EA, Heffron F. 1989. A *Salmonella* locus that controls resistance to microbicidal proteins from phagocytic cells. *Science* **243**:1059–1062. doi: [10.1126/science.2646710](https://doi.org/10.1126/science.2646710).
- Fields PI, Swanson RV, Haidaris CG, Heffron F. 1986. Mutants of *Salmonella* typhimurium that cannot survive within the macrophage are avirulent. *Proceedings of the National Academy of Sciences of USA* **83**:5189–5193. doi: [10.1073/pnas.83.14.5189](https://doi.org/10.1073/pnas.83.14.5189).
- Flanagan RS, Cosio G, Grinstein S. 2009. Antimicrobial mechanisms of phagocytes and bacterial evasion strategies. *Nature Reviews Microbiology* **7**:355–366. doi: [10.1038/nrmicro2128](https://doi.org/10.1038/nrmicro2128).
- Freeman JA, Ohl ME, Miller SI. 2003. The *Salmonella enterica* serovar typhimurium translocated effectors SseJ and SifB are targeted to the *Salmonella*-containing vacuole. *Infection and Immunity* **71**:418–427. doi: [10.1128/IAI.71.1.418-427.2003](https://doi.org/10.1128/IAI.71.1.418-427.2003).
- Galán JE, Curtiss R III. 1989. Virulence and vaccine potential of phoP mutants of *Salmonella* typhimurium. *Microbial Pathogenesis* **6**:433–443. doi: [10.1016/0882-4010\(89\)90085-5](https://doi.org/10.1016/0882-4010(89)90085-5).
- García Véscovi E, Soncini FC, Groisman EA. 1996. Mg²⁺ as an extracellular signal: environmental regulation of *Salmonella* virulence. *Cell* **84**:165–174. doi: [10.1016/S0092-8674\(00\)81003-X](https://doi.org/10.1016/S0092-8674(00)81003-X).
- Gerlach RG, Hölzer SU, Jäckel D, Hensel M. 2007. Rapid engineering of bacterial reporter gene fusions by using red recombination. *Applied and Environmental Microbiology* **73**:4234–4242. doi: [10.1128/AEM.00509-07](https://doi.org/10.1128/AEM.00509-07).
- Gibson DG, Young L, Chuang RY, Venter JC, Hutchison CA III, Smith HO. 2009. Enzymatic assembly of DNA molecules up to several hundred kilobases. *Nature Methods* **6**:343–345. doi: [10.1038/nmeth.1318](https://doi.org/10.1038/nmeth.1318).
- Goers Sweeney E, Henderson JN, Goers J, Wreden C, Hicks KG, Foster JK, Parthasarathy R, Remington SJ, Guillemin K. 2012. Structure and proposed mechanism for the pH-sensing *Helicobacter pylori* chemoreceptor TlpB. *Structure* **20**:1177–1188. doi: [10.1016/j.str.2012.04.021](https://doi.org/10.1016/j.str.2012.04.021).
- Groisman EA, Chiao E, Lipps CJ, Heffron F. 1989. *Salmonella* typhimurium phoP virulence gene is a transcriptional regulator. *Proceedings of the National Academy of Sciences of USA* **86**:7077–7081. doi: [10.1073/pnas.86.18.7077](https://doi.org/10.1073/pnas.86.18.7077).
- Gunn JS, Miller SI. 1996. PhoP-PhoQ activates transcription of pmrAB, encoding a two-component regulatory system involved in *Salmonella* typhimurium antimicrobial peptide resistance. *Journal of Bacteriology* **178**:6857–6864.

- Guo L**, Lim KB, Gunn JS, Bainbridge B, Darveau RP, Hackett M, Miller SI. 1997. Regulation of lipid A modifications by *Salmonella typhimurium* virulence genes phoP-phoQ. *Science* **276**:250–253. doi: [10.1126/science.276.5310.250](https://doi.org/10.1126/science.276.5310.250).
- Guo L**, Lim KB, Poduje CM, Daniel M, Gunn JS, Hackett M, Miller SI. 1998. Lipid A acylation and bacterial resistance against vertebrate antimicrobial peptides. *Cell* **95**:189–198. doi: [10.1016/S0092-8674\(00\)81750-X](https://doi.org/10.1016/S0092-8674(00)81750-X).
- Haraga A**, Ohlson MB, Miller SI. 2008. Salmonellae interplay with host cells. *Nature Reviews Microbiology* **6**:53–66. doi: [10.1038/nrmicro1788](https://doi.org/10.1038/nrmicro1788).
- Johnson BA**, Blevins RA. 1994. NMR view: a computer program for the visualization and analysis of NMR data. *Journal of Biomolecular NMR* **4**:603–614. doi: [10.1007/BF00404272](https://doi.org/10.1007/BF00404272).
- Kabsch W**. 2010. Xds. *Acta Crystallographica Section D, Biological Crystallography* **66**:125–132. doi: [10.1107/S0907444909047337](https://doi.org/10.1107/S0907444909047337).
- Kamal JK**, Nazeerunnisa M, Behere DV. 2002. Thermal unfolding of soybean peroxidase. Appropriate high denaturant concentrations induce cooperativity allowing the correct measurement of thermodynamic parameters. *The Journal of Biological Chemistry* **277**:40717–40721. doi: [10.1074/jbc.M208129200](https://doi.org/10.1074/jbc.M208129200).
- Karplus PA**, Diederichs K. 2012. Linking crystallographic model and data quality. *Science* **336**:1030–1033. doi: [10.1126/science.1218231](https://doi.org/10.1126/science.1218231).
- Lippa AM**, Goulian M. 2009. Feedback inhibition in the PhoQ/PhoP signaling system by a membrane peptide. *PLoS Genetics* **5**:e1000788. doi: [10.1371/journal.pgen.1000788](https://doi.org/10.1371/journal.pgen.1000788).
- Lippa AM**, Goulian M. 2012. Perturbation of the oxidizing environment of the periplasm stimulates the PhoQ/PhoP system in *Escherichia coli*. *Journal of Bacteriology* **194**:1457–1463. doi: [10.1128/JB.06055-11](https://doi.org/10.1128/JB.06055-11).
- Livak KJ**, Schmittgen TD. 2001. Analysis of relative gene expression data using real-time quantitative PCR and the 2(-Delta Delta C(T)) method. *Methods* **25**:402–408. doi: [10.1006/meth.2001.1262](https://doi.org/10.1006/meth.2001.1262).
- Martin-Orozco N**, Touret N, Zaharik ML, Park E, Kopelman R, Miller S, Finlay BB, Gros P, Grinstein S. 2006. Visualization of vacuolar acidification-induced transcription of genes of pathogens inside macrophages. *Molecular Biology of the Cell* **17**:498–510. doi: [10.1091/mbc.E04-12-1096](https://doi.org/10.1091/mbc.E04-12-1096).
- Mellman I**, Fuchs R, Helenius A. 1986. Acidification of the endocytic and exocytic pathways. *Annual Review of Biochemistry* **55**:663–700. doi: [10.1146/annurev.bi.55.070186.003311](https://doi.org/10.1146/annurev.bi.55.070186.003311).
- Miki T**, Okada N, Danbara H. 2004. Two periplasmic disulfide oxidoreductases, DsbA and SrgA, target outer membrane protein SpiA, a component of the *Salmonella* pathogenicity island 2 type III secretion system. *The Journal of Biological Chemistry* **279**:34631–34642. doi: [10.1074/jbc.M402760200](https://doi.org/10.1074/jbc.M402760200).
- Miller SI**, Kukral AM, Mekalanos JJ. 1989. A two-component regulatory system (phoP phoQ) controls *Salmonella typhimurium* virulence. *Proceedings of the National Academy of Sciences of USA* **86**:5054–5058. doi: [10.1073/pnas.86.13.5054](https://doi.org/10.1073/pnas.86.13.5054).
- Miller SI**, Mekalanos JJ. 1990. Constitutive expression of the phoP regulon attenuates *Salmonella* virulence and survival within macrophages. *Journal of Bacteriology* **172**:2485–2490.
- Molnar KS**, Bonomi M, Pellarin R, Clinthorne GD, Gonzalez G, Goldberg SD, Goulian M, Sali A, DeGrado WF. 2014. Cys-scanning disulfide crosslinking and bayesian modeling probe the transmembrane signaling mechanism of the histidine kinase, PhoQ. *Structure* **22**:1239–1251. doi: [10.1016/j.str.2014.04.019](https://doi.org/10.1016/j.str.2014.04.019).
- Montagne M**, Martel A, Le Moual H. 2001. Characterization of the catalytic activities of the PhoQ histidine protein kinase of *Salmonella enterica* serovar Typhimurium. *Journal of Bacteriology* **183**:1787–1791. doi: [10.1128/JB.183.5.1787-1791.2001](https://doi.org/10.1128/JB.183.5.1787-1791.2001).
- Müller S**, Götz M, Beier D. 2009. Histidine residue 94 is involved in pH sensing by histidine kinase ArsS of *Helicobacter pylori*. *PLOS ONE* **4**:e6930. doi: [10.1371/journal.pone.0006930](https://doi.org/10.1371/journal.pone.0006930).
- Núñez-Hernández C**, Tierrez A, Ortega AD, Pucciarelli MG, Godoy M, Eisman B, Casadesús J, García-del Portillo F. 2013. Genome expression analysis of nonproliferating intracellular *Salmonella enterica* serovar Typhimurium unravels an acid pH-dependent PhoP-PhoQ response essential for dormancy. *Infection and Immunity* **81**:154–165. doi: [10.1128/IAI.01080-12](https://doi.org/10.1128/IAI.01080-12).
- Perier A**, Chassaing A, Raffestin S, Pichard S, Masella M, Ménez A, Forge V, Chenal A, Gillet D. 2007. Concerted protonation of key histidines triggers membrane interaction of the diphtheria toxin T domain. *The Journal of Biological Chemistry* **282**:24239–24245. doi: [10.1074/jbc.M703392200](https://doi.org/10.1074/jbc.M703392200).
- Prost LR**, Daley ME, Bader MW, Klevit RE, Miller SI. 2008. The PhoQ histidine kinases of *Salmonella* and *Pseudomonas* spp. are structurally and functionally different: evidence that pH and antimicrobial peptide sensing contribute to mammalian pathogenesis. *Molecular Microbiology* **69**:503–519. doi: [10.1111/j.1365-2958.2008.06303.x](https://doi.org/10.1111/j.1365-2958.2008.06303.x).
- Prost LR**, Daley ME, Le Sage V, Bader MW, Le Moual H, Klevit RE, Miller SI. 2007. Activation of the bacterial sensor kinase PhoQ by acidic pH. *Molecular Cell* **26**:165–174. doi: [10.1016/j.molcel.2007.03.008](https://doi.org/10.1016/j.molcel.2007.03.008).
- Rathman M**, Sjaastad MD, Falkow S. 1996. Acidification of phagosomes containing *Salmonella typhimurium* in murine macrophages. *Infection and Immunity* **64**:2765–2773.
- Richards SM**, Strandberg KL, Conroy M, Gunn JS. 2012. Cationic antimicrobial peptides serve as activation signals for the *Salmonella* Typhimurium PhoPQ and PmrAB regulons in vitro and in vivo. *Frontiers in Cellular and Infection Microbiology* **2**:102. doi: [10.3389/fcimb.2012.00102](https://doi.org/10.3389/fcimb.2012.00102).
- Rosenberger CM**, Gallo RL, Finlay BB. 2004. Interplay between antibacterial effectors: a macrophage antimicrobial peptide impairs intracellular *Salmonella* replication. *Proceedings of the National Academy of Sciences of USA* **101**:2422–2427. doi: [10.1073/pnas.0304455101](https://doi.org/10.1073/pnas.0304455101).
- Sanowar S**, Martel A, Moual HL. 2003. Mutational analysis of the residue at position 48 in the *Salmonella enterica* Serovar Typhimurium PhoQ sensor kinase. *Journal of Bacteriology* **185**:935–941. doi: [10.1128/JB.185.6.1935-1941.2003](https://doi.org/10.1128/JB.185.6.1935-1941.2003).

- Schrodinger LL.** 2010. The PyMOL molecular Graphics system, Version 1.3r1.
- Shprung T, Peleg A, Rosenfeld Y, Trieu-Cuot P, Shai Y.** 2012. Effect of PhoP-PhoQ activation by broad repertoire of antimicrobial peptides on bacterial resistance. *The Journal of Biological Chemistry* **287**:4544–4551. doi: [10.1074/jbc.M111.278523](https://doi.org/10.1074/jbc.M111.278523).
- Vagin A, Teplyakov A.** 2010. Molecular replacement with MOLREP. *Acta Crystallographica Section D, Biological Crystallography* **66**:22–25. doi: [10.1107/S0907444909042589](https://doi.org/10.1107/S0907444909042589).
- Waldburger CD, Sauer RT.** 1996. Signal detection by the PhoQ sensor-transmitter. Characterization of the sensor domain and a response-impaired mutant that identifies ligand-binding determinants. *The Journal of Biological Chemistry* **271**:26630–26636. doi: [10.1074/jbc.271.43.26630](https://doi.org/10.1074/jbc.271.43.26630).
- Williamson DM, Elferich J, Ramakrishnan P, Thomas G, Shinde U.** 2013. The mechanism by which a propeptide-encoded pH sensor regulates spatiotemporal activation of furin. *The Journal of Biological Chemistry* **288**:19154–19165. doi: [10.1074/jbc.M112.442681](https://doi.org/10.1074/jbc.M112.442681).